GL-TR-90-0167

TGAL-90-05

(2)

Pg/Lg Discrimination in the Western United States

C. S. Lynnes
R. Baumstark
R. K. Cessaro
W. W. Chan

Teledyne Geotech Alexandria Laboratories
314 Montgomery Street
Alexandria, VA 22314-1581

10 June 1990

Scientific Report No. 2

APPROVED FOR PUBLIC RELEASE; DISTRIBUTION UNLIMITED

GEOPHYSICS LABORATORY
AIR FORCE SYSTEMS COMMAND
UNITED STATES AIR FORCE
HANSCOM AIR FORCE BASE, MASSACHUSETTS 01731-5000

SPONSORED BY
Defense Advanced Research Projects Agency
Nuclear Monitoring Research Office
ARPA ORDER NO 5307

MONITORED BY
Geophysics Laboratory
F19628-89-C-0063

The views and conclusions contained in this document are those of the authors and should not be interpreted as representing the official policies, either expressed or implied, of the Defense Advanced Research Projects Agency or the U.S. Government.

This technical report has been reviewed and is approved for publication.

JAMES F. LEWKOWICZ
Contract Manager
Solid Earth Geophysics Branch
Earth Sciences Division

JAMES F. LEWKOWICZ
Branch Chief
Solid Earth Geophysics Branch
Earth Sciences Division

FOR THE COMMANDER

DONALD H. ECKHARDT, Director
Earth Sciences Division

This report has been reviewed by the ESD Public Affairs Office (PA) and is releasable to the National Technical Information Service (NTIS).

Qualified requestors may obtain additional copies from the Defense Technical Information Center. All others should apply to the National Technical Information Service.

If your address has changed, or if you wish to be removed from the mailing list, or if the addressee is no longer employed by your organization, please notify GL/IMA, Hanscom AFB, MA 01731-5000. This will assist us in maintaining a current mailing list.

Do not return copies of this report unless contractual obligations or notices on a specific document requires that it be returned.

REPORT DOCUMENTATION PAGE

Form Approved
OMB No 0704 0188
Exp Date Jun 30 1986

1a REPORT SECURITY CLASSIFICATION **Unclassified**	1b RESTRICTIVE MARKINGS
2a SECURITY CLASSIFICATION AUTHORITY	3 DISTRIBUTION / AVAILABILITY OF REPORT **Approved for Public Release; Distribution Unlimited**
2b DECLASSIFICATION / DOWNGRADING SCHEDULE	
4 PERFORMING ORGANIZATION REPORT NUMBER(S) **TGAL-90-05**	5 MONITORING ORGANIZATION REPORT NUMBER(S) **GL-TR-90-0167**
6a NAME OF PERFORMING ORGANIZATION **Teledyne Geotech** — 6b OFFICE SYMBOL (*If applicable*)	7a NAME OF MONITORING ORGANIZATION **Geophysics Laboratory**
6c ADDRESS (*City, State, and ZIP Code*) **314 Montgomery Street** **Alexandria, VA 22314-1581**	7b ADDRESS (*City, State, and ZIP Code*) **Hanscom AFB, MA 01731-5000**
8a NAME OF FUNDING / SPONSORING ORGANIZATION **DARPA** — 8b OFFICE SYMBOL (*If applicable*) **NMRO**	9 PROCUREMENT INSTRUMENT IDENTIFICATION NUMBER **F19628-89-C-0063**
8c ADDRESS (*City, State, and ZIP Code*) **1400 Wilson Boulevard** **Arlington, VA 22209-2308**	10 SOURCE OF FUNDING NUMBERS

PROGRAM ELEMENT NO	PROJECT NO	TASK NO	WORK UNIT ACCESSION NO
62714E	**9A10**	**DA**	**AZ**

11 TITLE (*Include Security Classification*)
Pg/Lg Discrimination in the Western United States

12 PERSONAL AUTHOR(S)
C. S. Lynnes, R. Baumstark, R. K. Cessaro and W. W. Chan

13a TYPE OF REPORT	13b TIME COVERED	14 DATE OF REPORT (Year, Month, Day)	15 PAGE COUNT
Scientific #2	FROM **April 1989** TO **April 1990**	**1990 June 10**	**56**

16 SUPPLEMENTARY NOTATION

17 COSATI CODES			18 SUBJECT TERMS (*Continue on reverse if necessary and identify by block number*)
FIELD	GROUP	SUB-GROUP	**Explosion Discrimination, Crustal Phase Propagation**

19 ABSTRACT (*Continue on reverse if necessary and identify by block number*)

Various *P/Lg* ratios have been suggested by several workers as viable methods for discriminating explosions from earthquakes. However, the performance of these phase ratios as discriminants has been varied depending on the geographic region, the specific phases, and the frequency passband chosen for analysis. Recently installed networks capable of recording broadband and high-frequency digital data present the opportunity of using high-frequency data with possible improvements in discrimination performance.

In this study, we have measured *Pg/Lg* ratios over the frequency bands 0.5-1.0 Hz, 1-2 Hz, 2-4 Hz and 4-8 Hz for earthquakes and explosions in the western United States using GDSN data. Earthquake and explosion *Pg/Lg* ratios overlap almost completely for the 0.5-1.0 Hz band; at higher frequencies the *Pg/Lg* ratio for explosions increases, providing some separation. However, small explosions tend to look like earthquakes, perhaps due to their shallow depth. The explosion *Pg/Lg* ratios generally increase with increasing depth in most of the frequency bands studied, which may be due to an increase in source medium velocity with depth, increasing *Pg* amplitudes relative to *Lg*.

20 DISTRIBUTION / AVAILABILITY OF ABSTRACT	21 ABSTRACT SECURITY CLASSIFICATION
☐ UNCLASSIFIED/UNLIMITED ☐ SAME AS RPT ☐ DTIC USERS	**Unclassified**

22a NAME OF RESPONSIBLE INDIVIDUAL	22b TELEPHONE (*Include Area Code*)	22c OFFICE SYMBOL
James F. Lewkowicz	**(617) 377-3028**	**GL/LWH**

(19. Continued.)

The dominant factor in *Pg/Lg* ratios appears to be the propagation path. Earthquakes from southeastern California have systematically lower *Pg/Lg* ratios than do those from Nevada. Furthermore, the explosions have similar *Pg/Lg* ratios to the Nevada earthquakes in all frequency bands except 4-8 Hz. This suggests that for frequencies up to 4 Hz, the source-station path may be more important than the source type in determining the *Pg/Lg* ratio in this area, mitigating the efficacy of the *Pg/Lg* ratio as a discriminant. This is supported by a comparison of the *Pg/Lg* ratios of three explosions with their corresponding collapses. The *Pg/Lg* ratios of the explosions are quite similar to those of the collapses for most frequencies despite the differences in source function.

High frequency phase ratios offer some hope of discrimination, but at the cost of increased scatter and noise. Also, the California events show a distinct trend of increasing *Pg/Lg* with distance. This trend is accentuated at high frequencies, thus requiring a distance correction for effective discrimination.

EXECUTIVE SUMMARY

Various *P/Lg* ratios have been suggested by several workers as viable methods for discriminating explosions from earthquakes. However, the performance of these phase ratios as discriminants has been varied depending on the geographic region, the specific phases, and the frequency passband chosen for analysis. Recently installed networks capable of recording broadband and high-frequency digital data present the opportunity of using high-frequency data with possible improvements in discrimination performance.

In this study, we have measured *Pg/Lg* ratios over the frequency bands 0.5-1.0 Hz, 1-2 Hz, 2-4 Hz and 4-8 Hz for earthquakes and explosions in the western United States using GDSN data. Earthquake and explosion *Pg/Lg* ratios overlap almost completely for the 0.5-1.0 Hz band; at higher frequencies the *Pg/Lg* ratio for explosions increases, providing some separation. However, small explosions tend to look like earthquakes, perhaps due to their shallow depth. The explosion *Pg/Lg* ratios generally increase with increasing depth in most of the frequency bands studied, which may be due to an increase in source medium velocity with depth, increasing *Pg* amplitudes relative to *Lg*.

The dominant factor in *Pg/Lg* ratios appears to be the propagation path. Earthquakes from southeastern California have systematically lower *Pg/Lg* ratios than do those from Nevada. Furthermore, the explosions have similar *Pg/Lg* ratios to the Nevada earthquakes in all frequency bands except 4-8 Hz. This suggests that for frequencies up to 4 Hz, the source-station path may be more important than the source type in determining the *Pg/Lg* ratio in this area, mitigating the efficacy of the *Pg/Lg* ratio as a discriminant. This is supported by a comparison of the *Pg/Lg* ratios of three explosions with their corresponding collapses. The *Pg/Lg* ratios of the explosions are quite similar to those of the collapses for most frequencies despite

the differences in source function.

High frequency phase ratios offer some hope of discrimination, but at the cost of increased scatter and noise. Also, the California events show a distinct trend of increasing *Pg/Lg* with distance. This trend is accentuated at high frequencies, thus requiring a distance correction for effective discrimination.

Table of Contents

Executive Summary iii

List of Figures vi

List of Tables vii

Introduction 1

Data and Results 10

Methodology 10

Variation of *Pg/Lg* with Distance 13

Variation of *Pg/Lg* with Magnitude and Depth 16

Variation of *Pg/Lg* with Path 24

Comparison of Explosions and Collapses 30

Conclusion 33

Acknowledgements 34

References 35

List of Figures

Figure	*Page*
1. Sources and receiver used in study.	4
2. Example explosion and earthquake seismograms.	12
3. *Pg/Lg* vs. epicentral distance at 0.5-1.0 and 1-2 Hz.	14
4. *Pg/Lg* vs. epicentral distance at 2-4 and 4-8 Hz.	15
5. *Pg/Lg* vs. magnitude at 0.5-1.0 and 1-2 Hz.	18
6. *Pg/Lg* vs. magnitude at 2-4 and 4-8 Hz.	19
7. Explosion *Pg/Lg* vs. depth at 0.5-1.0 and 1-2 Hz.	20
8. Explosion *Pg/Lg* vs. depth at 2-4 and 4-8 Hz.	21
9. All *Pg/Lg* vs. depth at 0.5-1.0 and 1-2 Hz.	22
10. All *Pg/Lg* vs. depth at 2-4 and 4-8 Hz.	23
11. Variations in log(*Pg/Lg*) with location at 0.5-1.0 and 1-2 Hz.	27
12. Variations in log(*Pg/Lg*) with location at 2-4 and 4-8 Hz.	28
13. Maximum-likelihood averages of *Pg/Lg* for explosions and earthquakes.	29
14. Comparison of TAJO collapse and explosion *Pg* spectra.	31
15. Collapse and explosion *Pg/Lg* ratios vs. frequency.	32

List of Tables

Table	*Page*
1. Explosions used in this study.	5
2. Earthquakes used in this study.	6
3. Maximum-likelihood estimates of log(*Pg*/*Lg*) averages.	26

(THIS PAGE INTENTIONALLY LEFT BLANK)

INTRODUCTION

Some of the more promising means of discriminating between explosions and earthquakes involve the ratio of *P* waves to *Lg* or *S* waves. For example, Dysart and Pulli (1987) used *Pn/Sn* and *Pn/Lg* ratios to discriminate between regional earthquakes and mine blasts recorded at the NORESS array. With only a few exceptions, explosions had higher *Pn/Lg* ratios than earthquakes. The explosions also tended to have higher *Pn/Sn* ratios than the earthquakes. On the other hand, similar studies by Hutchenson and Kraft (1986) and Bennett and Murphy (1986) reported somewhat mediocre discrimination of explosions and earthquakes in the western U. S. by *P/Lg* ratios. Taylor *et al.* (1989) confirmed the latter results using the Lawrence Livermore National Laboratory (LLNL) broadband network. The reasons for the uneven performance of the *P/Lg* discriminant are unclear, but they are vital for the evaluation and application of the discriminant. A comprehensive review of early studies on *P/Lg* is given in Pomeroy *et al.* (1982).

Several factors may contribute to this uneven performance. The most obvious is the tectonic region: NORESS is located in the Precambrian Baltic shield area, and most of the sources in the Dysart and Pulli (1987) study occurred in the shield or in Paleozoic orogenic terranes. On the other other hand, the western U. S. studies involve source-station geometries located largely in the Tertiary basin-and-range and orogenic terranes. The large differences in crustal thickness, velocity structure and attenuation may be responsible for the differences between the studies. Another complication is the frequency: Hutchenson and Kraft (1986) measured *P/Lg* ratios for frequencies around 1 Hz, whereas the NORESS results used higher frequencies (3-12 Hz). Furthermore, a later study by Dysart and Pulli (1988) of NORESS data using intermediate frequencies was unsuccessful in discriminating earthquakes and

explosions. On the other hand, Taylor *et al.* (1989) found no significant difference between ~1 Hz and 6-8 Hz data for the LLNL broadband network in the western U. S.

One of the difficulties in determining why the discriminant fails is that the reasons for its success are still problematic. One obvious possibility is simply that explosions generate less shear energy than earthquakes for a given source size: the main sources of shear energy from explosions are $P \rightarrow S$ conversion at the free surface and scattering. Another possibility, proposed by Frankel (1989), is that the *P/Lg* ratio is a depth discriminant due to very high attenuation near the surface, where the explosions are detonated. Another possible explanation for the discriminant's apparent success is that the explosions in these studies generally come from a fairly limited area, which is often different from the source areas of the earthquakes, suggesting that the difference in *P/Lg* ratio between the two populations is due simply to path effects or near-source geology.

In this study, we have attempted to identify the reasons for the success/failure of the *P/Lg* discriminant in the western U. S. using seismograms recorded at the DWWSSN station JAS (Jamestown, California). We have selected earthquakes whose source-station paths are as similar as possible to those for the explosions, all of which were detonated at NTS (Figure 1). The events used are listed in Tables 1 and 2. We have also studied a wide range of frequencies in order to determine whether a particular frequency band provides significantly better or worse performance than others. Also, three pairs of explosions and their resultant collapses have been studied to eliminate the effect of propagation path on *P/Lg* ratios.

The primary results from this can be summarized as follows:

(1) The *Pg/Lg* ratio for explosions varies strongly as a function of source depth and size, so that smaller sources appear more nearly similar to earthquakes than do the

larger sources.

(2) The explosion *Pg/Lg* ratios are actually similar to earthquake *Pg/Lg* ratios along the same travel path, whereas both are quite different from earthquake *Pg/Lg* ratios along a significantly different path. This suggests that path effects are at least as important as source type in determining *Pg/Lg* ratios in the western U. S.

(3) In the highest frequency range studied, 4-8 Hz, the path effects seem to be diminished, and separation between explosions and earthquakes is improved over that in the lower frequency bands.

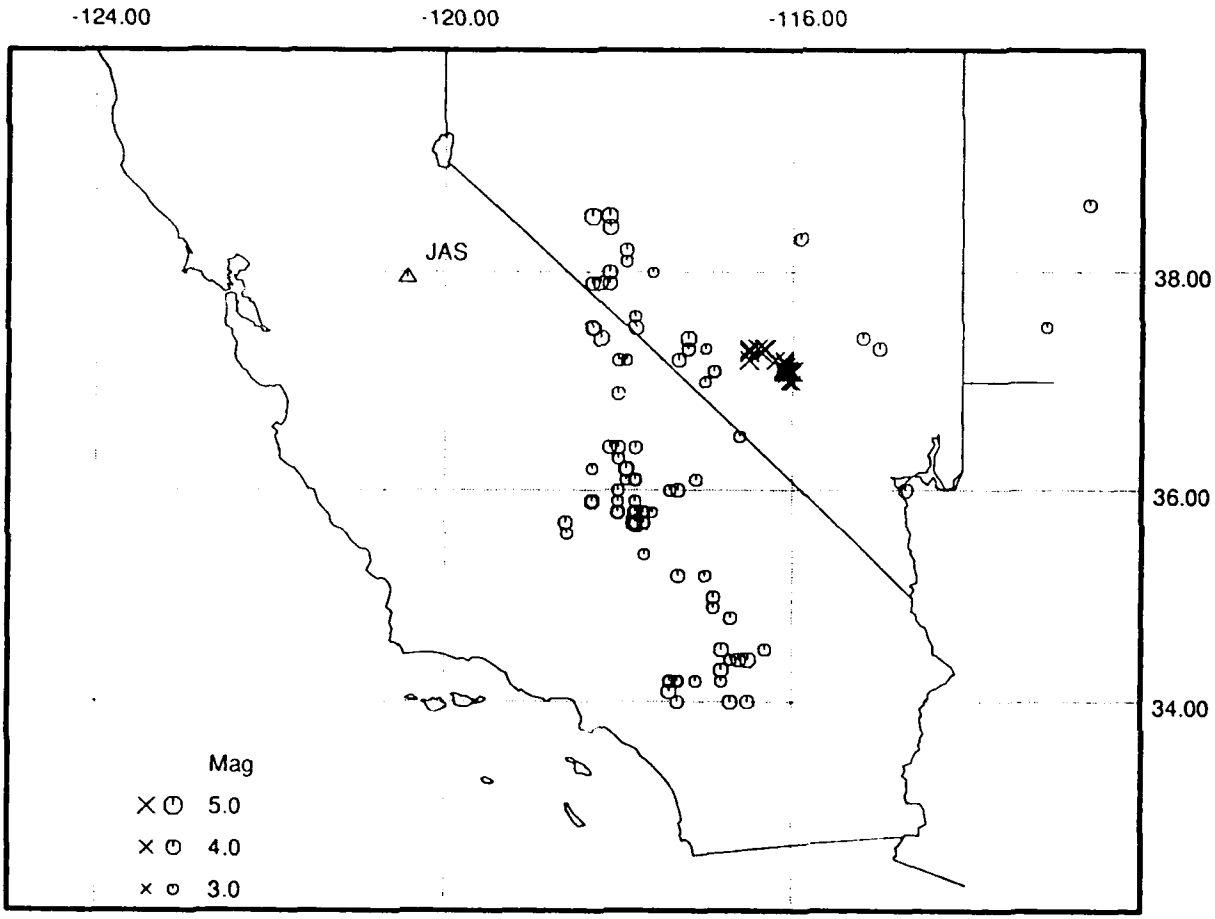

Figure 1. Sources and receiver used in the study. Octagons are earthquakes and X's are explosions.

Table 1. Explosions used in this study.

Date	Time	Latitude	Longitude	Depth	Magnitude	Name
14 NOV 1980	16:50:00	37.11	-116.02	0.320	4.5	DAUPHIN
17 DEC 1980	15:10:00	37.30	-116.30	0.573	5.0	SERPA
29 MAY 1981	16:00:00	37.10	-116.00	0.320	4.5	ALIGOTE
10 JUL 1981	14:00:00	37.13	-116.03	0.340	4.2	NIZA
16 JUL 1981	15:00:00	37.09	-116.02	0.204	3.3	PINEAU
27 AUG 1981	14:31:00	37.16	-116.07	0.294	4.3	ISLAY
24 SEP 1981	15:00:00	37.01	-116.02	0.213	3.5	CERNADA
1 OCT 1981	19:00:00	37.10	-116.00	0.472	5.2	PALIZA
11 NOV 1981	20:00:00	37.08	-116.07	0.445	5.0	TILCI
12 NOV 1981	15:00:00	37.10	-116.00	0.518	5.3	ROUSANNE
3 DEC 1981	15:00:00	37.15	-116.07	0.494	4.9	AKAVI
16 DEC 1981	21:05:00	37.12	-116.12	0.335	4.4	CABOC
28 JAN 1982	16:00:00	37.10	-116.10	0.640	5.8	JORNADA
29 JUL 1982	20:05:00	37.10	-116.08	0.400	4.6	MONTEREY
5 AUG 1982	14:00:00	37.10	-116.00	0.640	5.4	ATRISCO
2 SEP 1982	14:00:00	37.02	-116.02	0.229	3.3	CERRO
23 SEP 1982	16:00:00	37.20	-116.20	0.408	4.8	HURONLANDING/ DIAMONDACE
23 SEP 1982	17:00:00	37.20	-116.10	0.451	4.8	FRISCO
29 SEP 1982	13:30:00	37.09	-116.05	0.564	4.1	BORREGO
12 NOV 1982	19:17:00	37.02	-116.03	0.366	4.3	SEYVAL
11 FEB 1983	16:00:00	37.10	-116.00	0.304	4.1	COALORA
17 FEB 1983	17:00:00	37.16	-116.06	0.343	4.0	CHEEDAM
26 MAY 1983	15:00:00	37.10	-116.00	0.384	4.4	FAHADA
9 JUN 1983	17:10:00	37.16	-116.09	0.320	4.6	DANABLU
3 AUG 1983	13:33:00	37.12	-116.09	0.326	4.3	LABAN
11 AUG 1983	14:00:00	37.00	-116.00	0.320	4.2	SABADO
22 SEP 1983	15:00:00	37.11	-116.05	0.533	4.1	TECHADO
31 JAN 1984	15:30:00	37.11	-116.12	0.388	4.4	GORBEA
20 JUN 1984	15:15:00	37.00	-116.00	0.381	4.5	DUORO
2 AUG 1984	15:00:00	37.00	-116.00	0.335	4.4	CORREO
30 AUG 1984	14:45:00	37.09	-116.00	0.366	4.3	DOLCETTO
13 SEP 1984	14:00:00	37.10	-116.10	0.483	5.0	BRETON
23 MAR 1985	18:30:00	37.18	-116.09	0.515	5.1	COTTAGE
6 APR 1985	23:15:00	37.20	-116.20	0.000	4.8	MISTYRAIN
12 JUN 1985	17:30:00	37.10	-116.10	0.293	4.2	VILLE
26 JUN 1985	18:03:00	37.12	-116.12	0.381	4.0	MARIBO
17 AUG 1985	16:25:00	37.00	-116.04	0.332	4.2	CHAMITA
16 OCT 1985	21:35:00	37.11	-116.12	0.415	4.6	ROQUEFORT
22 MAR 1986	16:15:00	37.10	-116.10	0.610	5.0	GLENCOE
10 APR 1986	14:08:30	37.20	-116.20	0.400	4.9	MIGHTYOAK
21 MAY 1986	13:59:00	37.13	-116.06	0.500	3.9	PANAMINT
5 JUN 1986	15:04:00	37.10	-116.02	0.500	5.3	TAJO
24 JUL 1986	15:05:00	37.10	-116.10	0.400	4.4	CORNUCOPIA

Table 2. Earthquakes used in this study.

Date	Time	Latitude	Longitude	Depth	Magnitude
2 OCT 1980	01:48:13	37.30	-117.00	5	3.0
18 OCT 1980	03:54:30	34.40	-116.70	8	3.4
19 OCT 1980	22:59:52	34.40	-116.70	9	3.1
13 DEC 1980	04:10:16	35.90	-118.00	5	3.1
13 DEC 1980	14:15:47	34.50	-116.30	5	3.4
29 DEC 1980	07:12:53	37.50	-113.10	7	3.1
2 MAY 1981	02:11:05	35.90	-117.80	5	3.2
5 MAY 1981	13:59:05	36.40	-118.10	1	3.8
5 MAY 1981	14:34:52	36.40	-118.00	1	3.7
18 MAY 1981	21:32:48	37.20	-117.90	6	3.1
23 MAY 1981	18:50:21	36.10	-117.90	1	3.1
11 JUN 1981	18:00:43	38.30	-115.90	5	3.6
5 JUL 1981	10:30:48	35.80	-117.70	5	3.1
5 JUL 1981	12:31:00	35.80	-117.70	5	3.0
5 JUL 1981	13:33:50	35.80	-117.70	5	3.0
5 JUL 1981	17:45:24	35.80	-117.70	7	3.0
25 JUL 1981	20:05:54	36.10	-117.80	6	3.0
23 AUG 1981	04:32:29	38.00	-117.60	6	3.0
12 SEP 1981	21:23:07	34.20	-117.30	7	3.6
16 SEP 1981	07:57:42	34.20	-117.30	4	3.0
13 OCT 1981	14:47:53	37.10	-116.90	6	3.4
13 OCT 1981	19:51:12	37.00	-117.00	5	3.1
15 OCT 1981	04:21:10	37.10	-116.90	1	3.5
11 NOV 1981	20:25:10	35.80	-117.70	7	3.2
19 NOV 1981	21:40:53	37.10	-116.90	6	3.1
24 NOV 1981	09:20:17	34.80	-116.70	6	3.5
16 DEC 1981	01:34:52	36.20	-117.90	3	3.5
24 JAN 1982	15:44:07	37.50	-117.80	5	4.1
28 JAN 1982	22:51:02	38.50	-118.10	5	4.5
31 JUL 1982	00:57:58	35.80	-117.70	5	3.2
14 AUG 1982	02:37:59	34.20	-117.30	5	3.1
2 SEP 1982	22:51:06	38.10	-117.90	5	3.2
25 SEP 1982	23:29:46	36.40	-117.80	5	3.5
28 SEP 1982	10:43:51	35.80	-117.80	5	3.5
28 SEP 1982	17:35:05	35.80	-117.80	9	3.1
29 SEP 1982	18:19:16	35.80	-117.80	6	3.9
29 SEP 1982	18:21:01	35.80	-117.80	8	4.2
29 SEP 1982	19:37:14	35.80	-117.80	9	3.8
30 SEP 1982	22:38:10	35.80	-117.80	8	4.1
1 OCT 1982	01:33:35	37.90	-118.20	5	3.9
1 OCT 1982	06:24:58	35.80	-117.80	4	3.1
1 OCT 1982	09:21:16	35.80	-117.80	4	3.2
1 OCT 1982	12:19:32	35.70	-117.80	5	3.4
1 OCT 1982	17:14:42	35.80	-117.80	8	3.8

Table 2. Earthquakes used in this study.

Date	Time	Latitude	Longitude	Depth	Magnitude
1 OCT 1982	20:01:26	35.80	-117.80	8	3.1
1 OCT 1982	20:45:55	35.80	-117.70	6	3.7
1 OCT 1982	20:46:03	35.80	-117.70	6	3.8
1 OCT 1982	21:14:13	35.70	-117.70	5	3.1
1 OCT 1982	22:10:21	35.70	-117.80	7	4.3
2 OCT 1982	09:33:05	37.90	-118.30	5	3.7
2 OCT 1982	14:01:56	35.80	-117.70	6	3.5
2 OCT 1982	16:01:21	35.80	-117.80	8	3.5
3 OCT 1982	09:47:42	35.80	-117.80	5	3.0
4 OCT 1982	02:23:59	37.90	-118.10	5	3.9
4 OCT 1982	18:43:28	35.80	-117.80	8	3.9
6 OCT 1982	11:38:40	35.80	-117.60	4	3.0
7 OCT 1982	15:50:05	35.70	-117.70	5	3.2
7 OCT 1982	17:54:36	35.70	-117.70	10	3.9
12 OCT 1982	08:22:46	35.80	-117.70	8	3.7
12 OCT 1982	17:32:31	35.80	-117.70	9	3.1
21 OCT 1982	19:23:35	35.70	-117.70	6	3.3
29 OCT 1982	09:20:20	35.70	-117.70	6	3.2
30 OCT 1982	14:43:13	35.70	-117.80	7	3.1
10 NOV 1982	11:21:25	34.00	-116.70	8	3.9
12 NOV 1982	05:26:47	38.00	-118.10	5	3.9
1 JAN 1983	04:12:21	35.80	-117.70	6	3.0
2 JAN 1983	16:32:19	36.50	-116.60	5	3.2
3 JAN 1983	17:39:43	36.50	-116.60	5	3.1
5 JAN 1983	09:17:16	37.60	-117.80	6	3.2
5 JAN 1983	16:06:34	35.70	-117.80	8	3.0
6 JAN 1983	20:30:51	35.80	-117.70	7	3.0
7 JAN 1983	13:43:43	35.70	-117.80	7	3.9
7 JAN 1983	14:03:22	35.80	-117.70	6	3.0
7 JAN 1983	14:19:55	35.70	-117.80	9	3.0
7 JAN 1983	18:15:32	35.80	-117.80	6	3.1
7 JAN 1983	19:22:32	35.80	-117.80	9	3.0
8 JAN 1983	07:19:30	34.10	-117.40	5	4.1
8 JAN 1983	07:30:58	35.70	-117.80	9	3.3
8 JAN 1983	13:26:30	35.80	-117.70	6	3.1
13 JAN 1983	15:00:59	35.70	-117.80	9	3.0
17 JAN 1983	01:09:00	35.70	-118.60	7	3.7
1 FEB 1983	22:09:07	35.80	-117.70	11	3.1
23 FEB 1983	11:10:20	36.00	-114.70	5	3.9
1 MAR 1983	01:49:16	35.80	-117.70	6	3.3
2 MAR 1983	14:23:55	35.80	-117.70	10	3.2
4 MAR 1983	05:51:20	35.80	-117.70	10	3.0
11 MAR 1983	05:26:29	35.80	-117.70	10	3.1
21 MAY 1983	11:02:31	36.10	-117.10	5	3.4

Table 2. Earthquakes used in this study.

Date	Time	Latitude	Longitude	Depth	Magnitude
4 JUN 1983	11:37:40	37.40	-115.20	6	3.6
15 JUL 1983	22:03:10	38.50	-118.30	13	4.6
18 JUL 1983	04:36:47	34.20	-117.10	3	3.2
12 SEP 1983	12:08:02	34.00	-117.30	15	3.6
12 SEP 1983	21:33:35	35.20	-117.00	6	3.2
23 SEP 1983	01:35:26	35.60	-118.60	2	3.2
19 OCT 1983	14:00:37	35.90	-118.30	5	4.2
19 OCT 1983	19:48:24	35.90	-118.30	5	3.8
30 OCT 1983	20:02:59	35.90	-118.30	5	3.9
6 NOV 1983	01:34:31	35.90	-118.30	1	3.1
6 NOV 1983	02:08:1[illegible]	35.90	-118.30	0	3.1
9 DEC 1983	08:58:41	38.60	-112.60	7	3.6
18 DEC 1983	17:56:48	35.80	-118.00	4	3.3
29 DEC 1983	07:23:29	35.90	-118.30	1	3.3
29 DEC 1983	19:46:16	34.20	-117.40	8	3.6
29 DEC 1983	19:49:13	34.20	-117.40	6	2.9
29 DEC 1983	19:50:02	34.20	-117.30	8	2.7
12 JAN 1984	15:47:16	35.90	-118.30	1	3.1
16 JAN 1984	04:06:12	35.90	-118.30	0	3.4
20 JAN 1984	08:38:49	36.20	-118.30	6	3.1
20 JAN 1984	12:07:50	36.00	-118.00	9	3.3
11 JUN 1984	22:21:10	34.40	-116.60	2	4.0
17 JUN 1984	20:23:24	38.20	-117.90	6	3.8
19 AUG 1984	02:22:34	38.40	-118.10	5	4.2
7 SEP 1984	14:51:51	36.00	-117.30	0	3.7
2 JAN 1985	05:24:58	34.00	-116.50	9	3.8
8 JAN 1985	06:59:38	36.90	-118.00	5	3.6
1 APR 1985	06:13:33	36.00	-117.40	0	3.2
13 MAY 1985	21:24:00	35.80	-117.70	6	3.4
10 JUN 1985	00:58:01	34.20	-116.80	11	3.3
18 JUN 1985	01:23:40	35.20	-117.30	8	3.8
16 JUL 1985	17:57:50	34.50	-116.80	0	3.9
6 AUG 1985	03:45:36	35.40	-117.70	12	3.1
14 AUG 1985	06:12:56	35.00	-116.90	8	3.6
16 AUG 1985	01:51:21	36.20	-117.90	5	4.3
19 AUG 1985	23:10:26	34.90	-116.90	6	3.2
29 AUG 1985	07:59:08	34.30	-116.80	5	4.0
2 SEP 1985	19:45:08	37.20	-118.00	5	3.4
10 DEC 1985	06:10:25	37.30	-115.00	5	3.7
16 DEC 1985	09:09:52	36.30	-118.00	6	3.2
2 MAR 1986	23:03:01	35.90	-118.30	6	3.2
6 MAR 1986	20:16:52	37.20	-117.30	5	3.7
21 APR 1986	06:35:59	35.80	-117.80	4	3.3
23 MAY 1986	11:41:55	35.80	-118.00	10	3.9

Table 2. Earthquakes used in this study.

Date	Time	Latitude	Longitude	Depth	Magnitude
4 JUN 1986	15:07:38	37.30	-117.20	5	3.5
18 JUL 1986	17:00:36	36.10	-117.80	1	3.7
18 JUL 1986	17:02:50	36.10	-117.80	3	3.4
21 JUL 1986	20:40:25	37.50	-118.30	10	3.6
21 JUL 1986	23:43:04	37.50	-118.30	10	4.1
22 JUL 1986	18:19:36	37.50	-118.30	10	4.2
24 JUL 1986	14:58:45	37.50	-118.30	10	3.7
27 JUL 1986	03:49:40	37.40	-118.20	10	4.2
19 AUG 1986	20:38:47	37.50	-118.30	10	3.5
24 SEP 1986	14:20:33	37.40	-117.20	5	4.3
24 SEP 1986	14:35:55	37.40	-117.20	5	4.3

DATA AND RESULTS

Methodology

The first station studied was JAS (Jamestown, California), due to its long digital history and large number of recorded events from the Nevada Test Site and the California-Nevada border region. The station was moved in 1984 and renamed JAS1, but since this later site is less than 3 km away, both data sets are considered together. The events were selected in order to minimize the differences in epicentral distance and azimuth in an effort to limit the effect of gross path differences (Figure 1). Since well recorded explosions in this area were basically limited to the Nevada Test site, all such explosions were used. Earthquakes were chosen to be as close to NTS as possible.

The seismograms were processed by picking the onset of the *Pg* and *Lg* phases and measuring the *Pg/Lg* ratio in the frequency bands 0.5-1.0 Hz, 1-2 Hz, 2-4 Hz, 3-6 Hz, and 4-8 Hz. An example of both earthquake and explosion seismograms is shown in Figure 2, bandpassed in several of these frequency bands. The explosion actually generates substantial low-frequency *Lg* energy, resulting in a *Pg/Lg* ratio that is less than that of the earthquake in the 0.5-1.0 Hz band. As the frequency increases, however, the explosion *Lg* energy drops precipitously, resulting in a *Pg/Lg* ratio that is higher than that of the earthquake in the highest frequency band.

One spectral-domain and three time-domain measurement methods were tried, in an effort to find the most stable and/or effective method of computing phase ratios. In the spectral-domain method, 12.8 second windows were extracted, starting 1.3 seconds before the arrival onset, and cosine tapers were applied to the first 10% and last 10% of the window. Noise windows before the *Pg* onset and immediately prior to the *Lg* onset were also extracted.

The *Lg* "noise" window actually consists largely of *Pg* coda. Spectral amplitudes were obtained by applying a Hartley transform (Bracewell, 1986) to the windows, and instrument corrections were applied. A geometric mean over the frequency band of interest was then computed.

For the time-domain measurements, the seismograms were filtered with a zero-phase six-pole Butterworth bandpass filter over the frequency band of interest. Three types of time-domain measurements were then obtained from the 10 second windows starting at the arrival onset:

(1) the root-mean-square (RMS) of the window

(2) the maximum zero-to-peak amplitude within the window, and

(3) the range of the maximum peak to maximum trough within the window.

The latter two time-domain methods proved to be somewhat unstable at high frequencies: even small glitches in the seismograms, difficult to remove with conventional despiking algorithms, produce anomalously large amplitudes in the higher passbands. These glitches also affect the spectral and the time-domain RMS methods, but the effects are mitigated by the averaging nature of these methods. In the large, the results were similar to the spectral domain method, although the latter two time-domain methods seemed to show somewhat more scatter. (The RMS method is analogous to the spectral method without instrument correction.) Throughout the rest of the paper, the results will be those obtained with the spectral-domain method.

The noise windows are important for assessing the quality of a *Pg/Lg* ratio. In cases where the *Pg* signal/noise amplitude ratio is less than 1.4 (corresponding to a signal/noise power ratio of 2), while the *Lg* signal/noise amplitude ratio is greater than 1.4, the *Pg/Lg* ratio

is actually an upper bound. In cases where the *Pg* signal/noise is greater than 1.4, while the *Lg* signal/noise is less than 1.4, the *Pg/Lg* ratio is a lower bound. (In cases where both signal/noise ratios were less than 1.4, the datum was discarded.) A lower-bound value can be used in discrimination if it falls above the discrimination threshold, and an upper-bound value can be useful if it falls below the threshold.

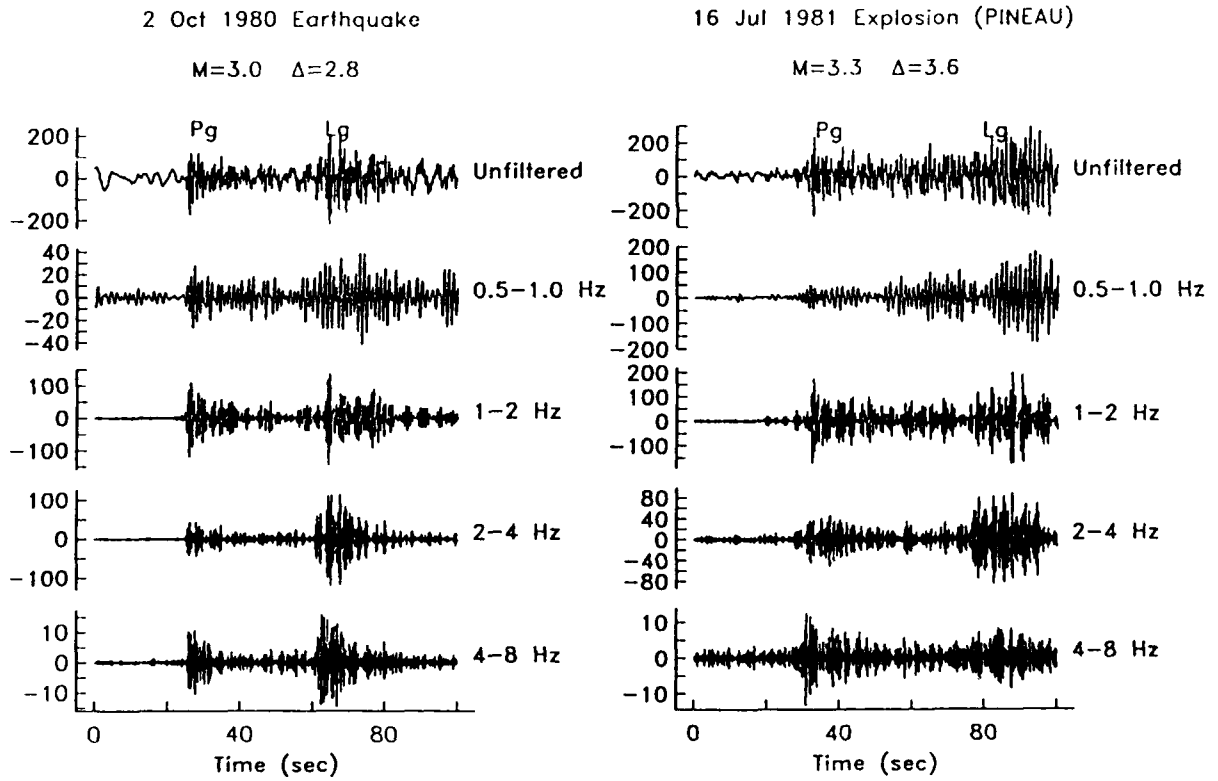

Figure 2. Example seismograms from an earthquake and explosion of similar size and distance from JAS. The top trace is unfiltered; the lower traces are filtered using a six-pole zero-phase Butterworth bandpass filter.

Variation of *Pg/Lg* with Distance

The *Pg/Lg* ratios for all events in four frequency bands are shown plotted against source-station distance in Figures 3 and 4. In all of the frequency bands, the average *Pg/Lg* ratio for explosions is higher than that of the earthquakes. However, the explosion and earthquake populations exhibit an extensive overlap in the lowest frequency band. As the frequency increases, the overlap diminishes somewhat, so that the two populations do show a fair degree of separation in the highest frequency band. Despite the still incomplete separation, the *Pg/Lg* ratio in the 4-8 Hz band is nevertheless useful in that only 5% of the explosions have *Pg/Lg* ratios below 0.8, while only 2% of the earthquakes have *Pg/Lg* ratios above 1.5. About ¼ of the events fall into the intermediate range.

One possible explanation of the overlap is a simple obfuscation of explosion *Lg* by the *Pg* coda. In general, however, both the low explosion *Pg/Lg* ratios and the high earthquake *Pg/Lg* ratios tend to be uncensored values (*i.e.*, both *Pg* and *Lg* have a signal/noise ratio greater than 1.4).

Due to the different propagation characteristics of *Pg* and *Lg*, including both attenuation and geometric spreading, it is reasonable to expect some trends with distance. The scatter of the data is generally too great to discern well defined trends. However, as the frequency increases, the *Pg/Lg* ratio does appear to show a general increase with distance. As will be shown later, this trend is accentuated by separating the ratios according to the source-station path.

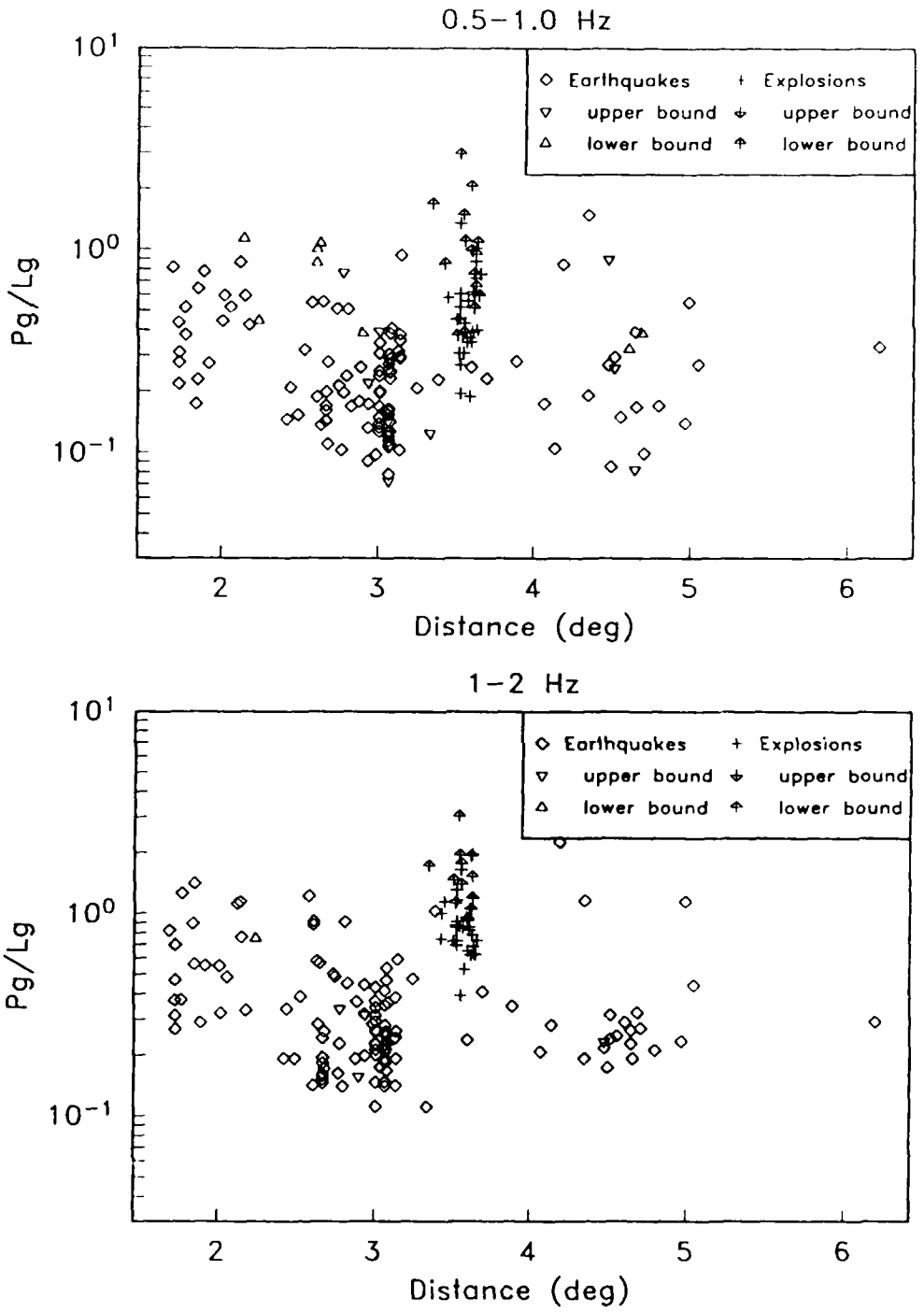

Figure 3. *Pg/Lg* ratios plotted vs. epicentral distance for the 0.5-1.0 Hz and 1-2 Hz bands. Explosions are shown as crosses (uncensored values) and arrows (upper and lower bound values). Earthquakes are shown as diamonds (uncensored values) and triangles (upper and lower bound values).

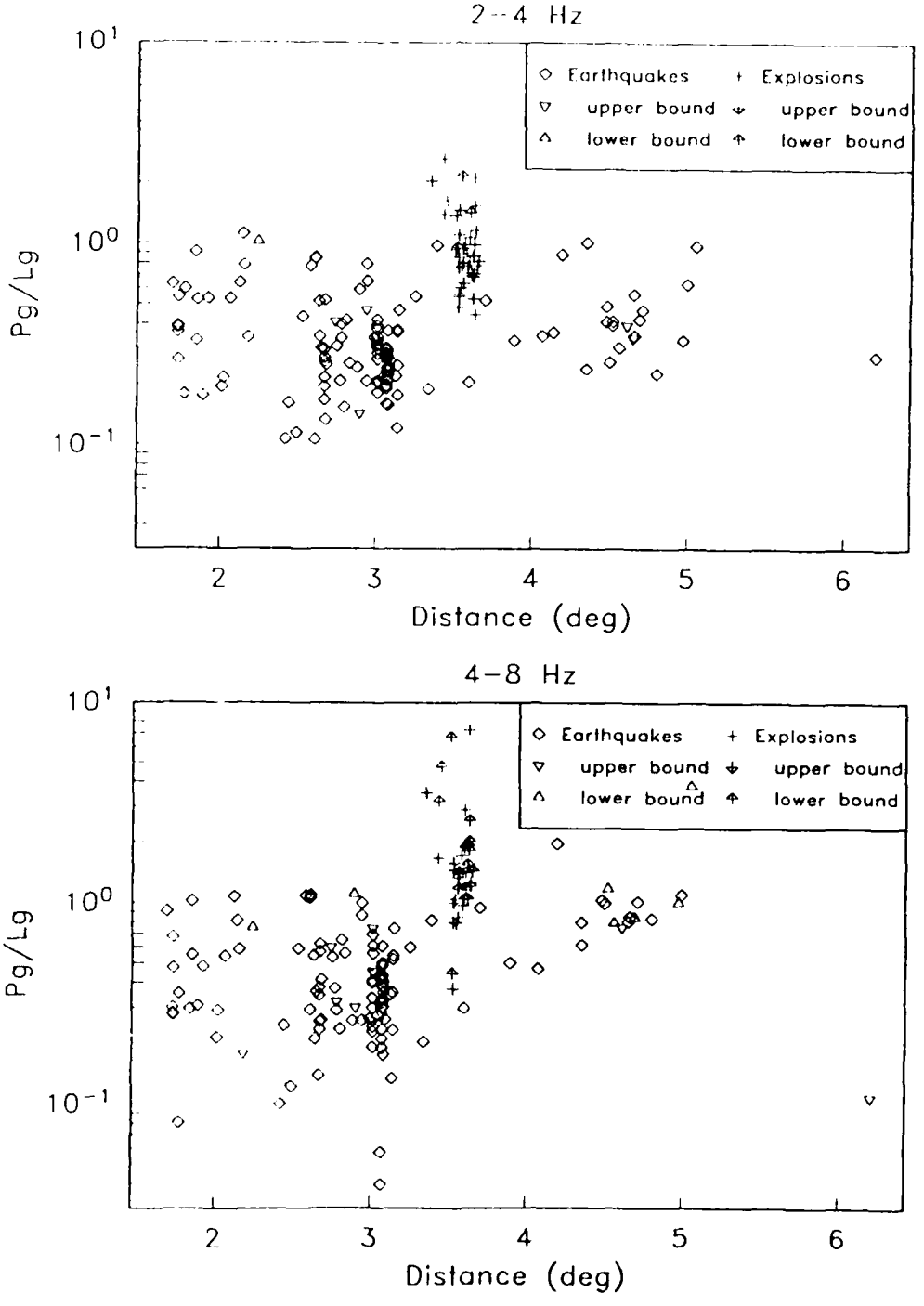

Figure 4. Same as Figure 3 for 2-4 Hz and 4-8 Hz bands.

Variation of *Pg/Lg* with Magnitude and Depth

The *Pg/Lg* ratios are plotted against the source magnitude in Figures 5 and 6. The magnitudes are NEIC body-wave magnitudes, if available. If they are not available, local magnitudes are shown. For all frequency bands, the explosion *Pg/Lg* ratios increase with magnitude, whereas the earthquake *Pg/Lg* ratios show no apparent trend in any frequency band. The result is that small explosions tend to resemble earthquakes insofar as their *Pg/Lg* ratios are concerned. In fact, part of the separation in explosion and earthquake populations in Figures 3 and 4 is due to a magnitude bias between the two groups.

The trend of increasing explosion *Pg/Lg* ratios with magnitude was also noted by Taylor *et al.* (1989). As one might expect from the strong correlation between explosion size and depth, *Pg/Lg* for explosions also increases with increasing depth (Figures 7 and 8) in three out of the four frequency bands. This was also noted by Taylor *et al.* for ~1 Hz data for the LLNL network, who observed that the trend seemed to disappear at depths below 1 km. There does not appear to be a similar relationship between *Pg/Lg* and depth for earthquakes (Figures 9 and 10). However, the depths, which are obtained from NEIC, are probably not reliable enough to conclude that there is no relationship between *Pg/Lg* and depth for earthquakes.

One possible explanation for the increase of *Pg/Lg* with depth might be *pP* interference with *Pg*. However, the shallower explosions in particular should be unaffected by *pP* interference in the 0.5-1.0 Hz band. Another possibility is differential contributions from *S** to the *Pg* and *Lg* wavetrains, but this effect should be minimal at high frequencies. Thus, the former explanation may explain the trend in the high frequency bands, but not the lowest, while the latter may explain the lowest band but not the higher. Perhaps the simplest expla-

nation is that the shallower explosions are detonated in lower velocity media. Lower velocities constrict the cone of rays contributing to *Pg* and thus the proportion of energy radiated as *Pg*. Furthermore, Lilwall (1988) and Frankel (1989) have shown that the lower velocities near the surface also tend to increase *Lg* generation, an effect which increases with increasing frequency. In any case, the source depth (or magnitude) appears to be a crucial factor in determining the *Pg/Lg* ratio.

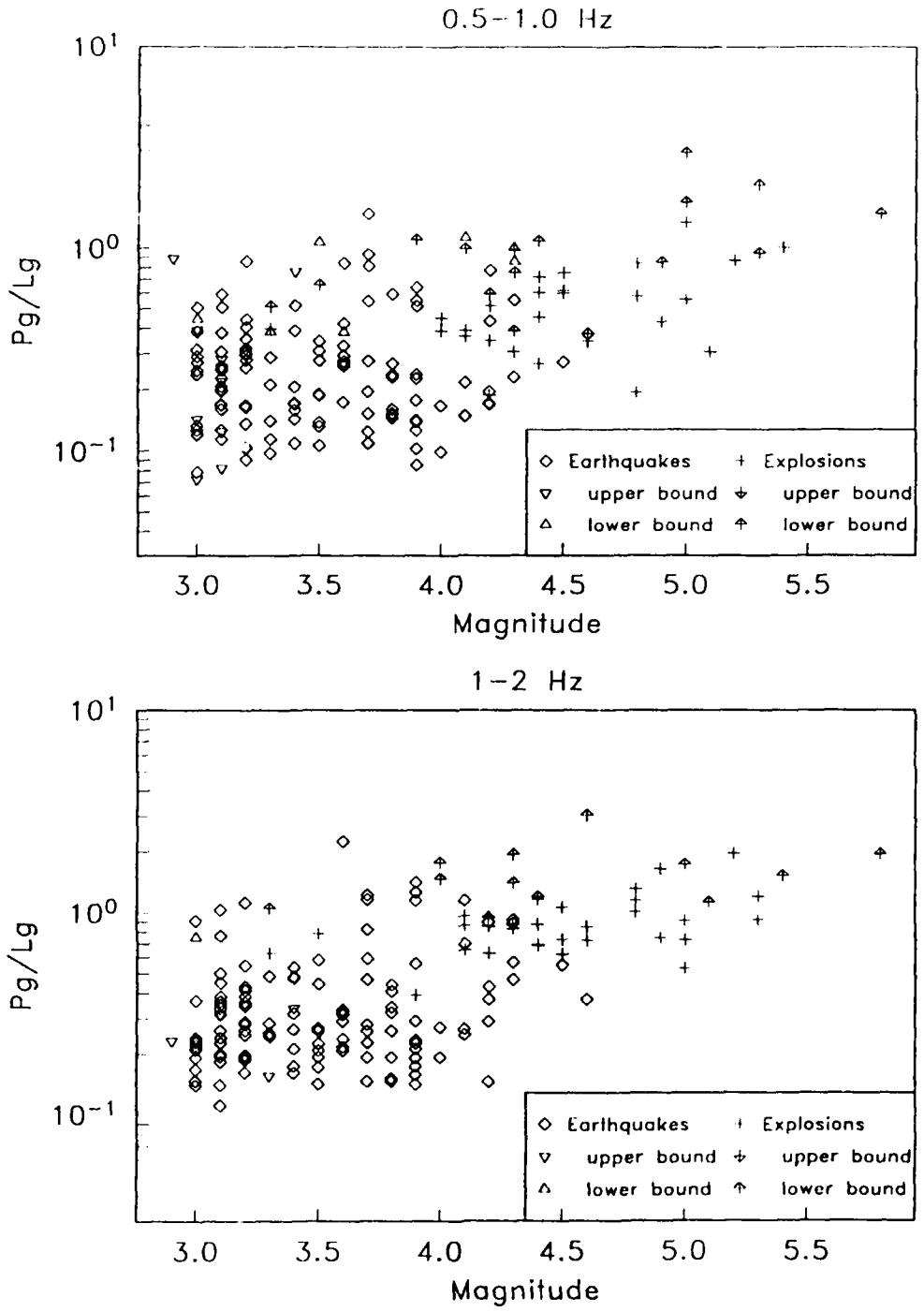

Figure 5. *Pg/Lg* ratios plotted vs. magnitude for the 0.5-1.0 Hz and 1-2 Hz bands. Symbols are the same as in Figure 3.

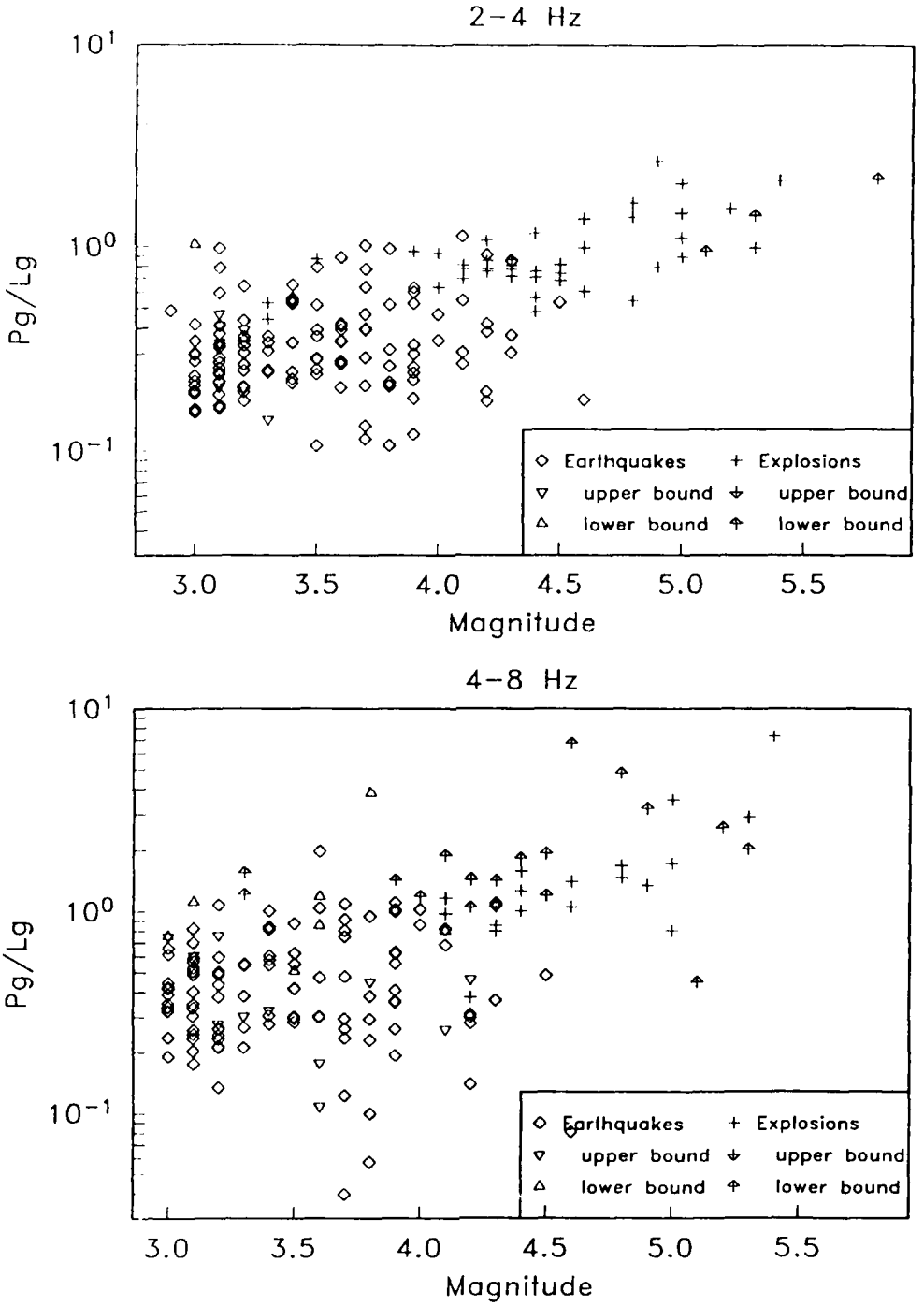

Figure 6. Same as Figure 5 for the 2-4 Hz and 4-8 Hz bands.

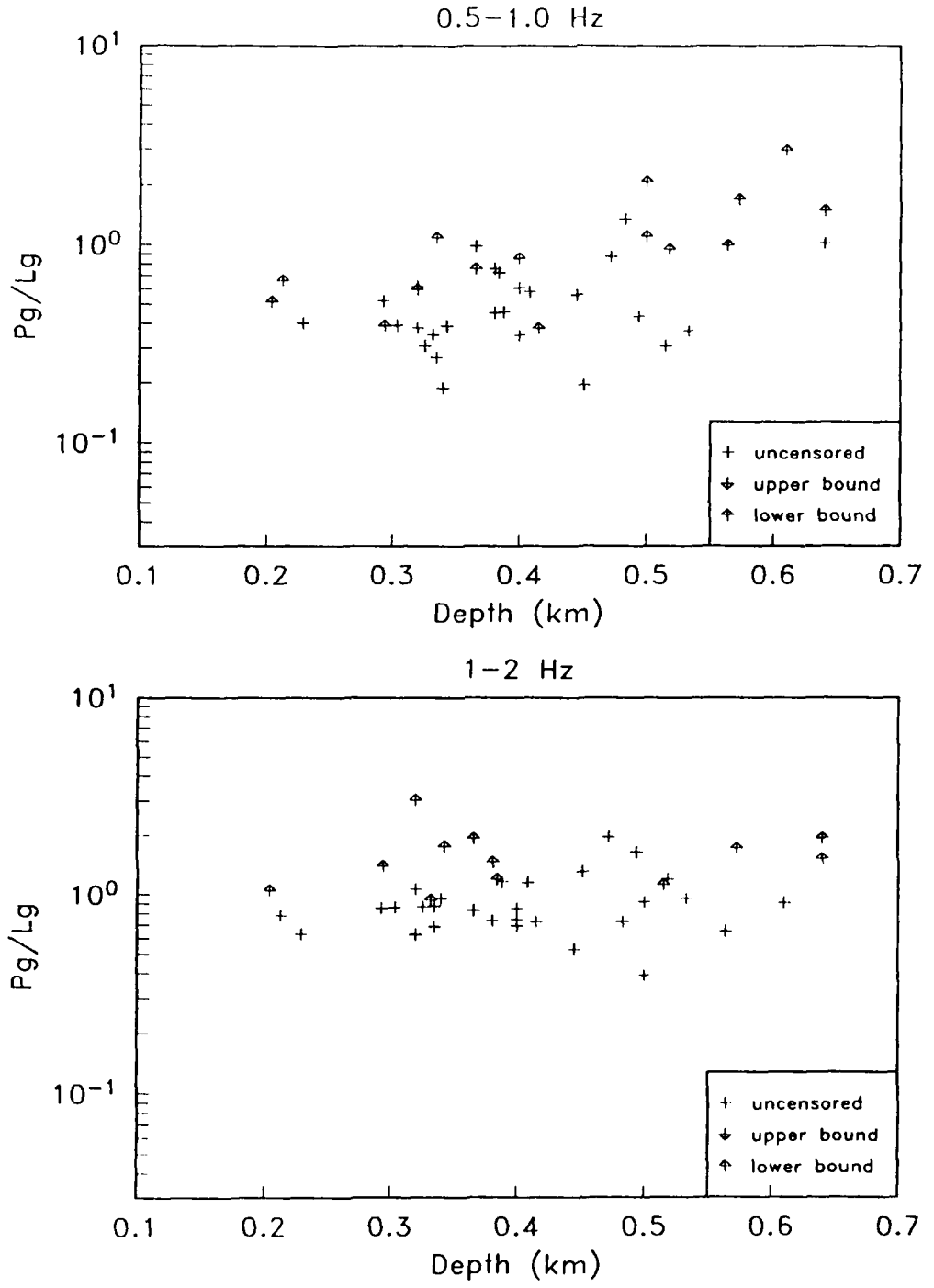

Figure 7. Explosion *Pg/Lg* ratios for the 0.5-1.0 Hz and 1-2 Hz band plotted vs. burial depth.

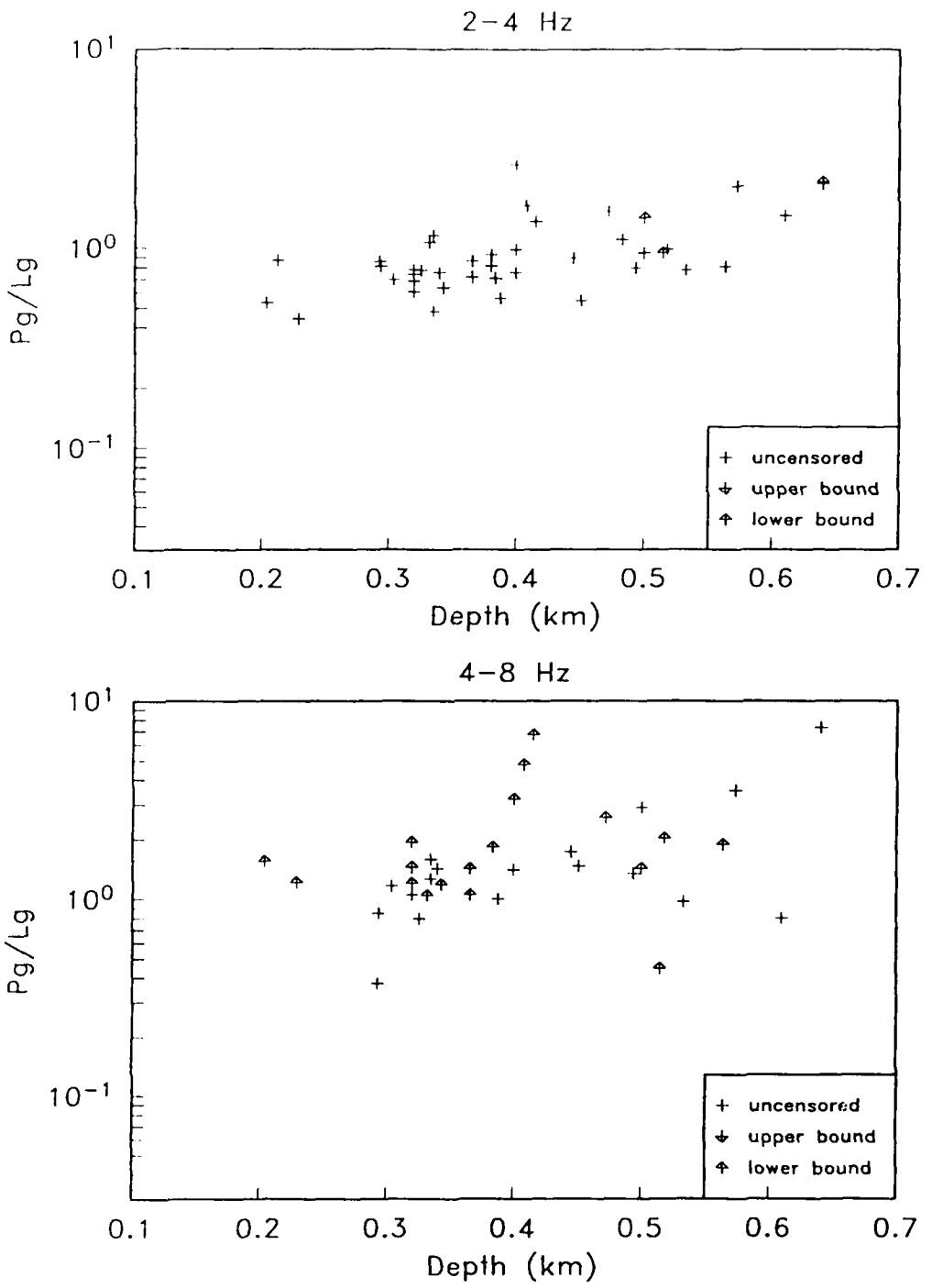

Figure 8. Same as Figure 7 for the 2-4 Hz and 4-8 Hz bands.

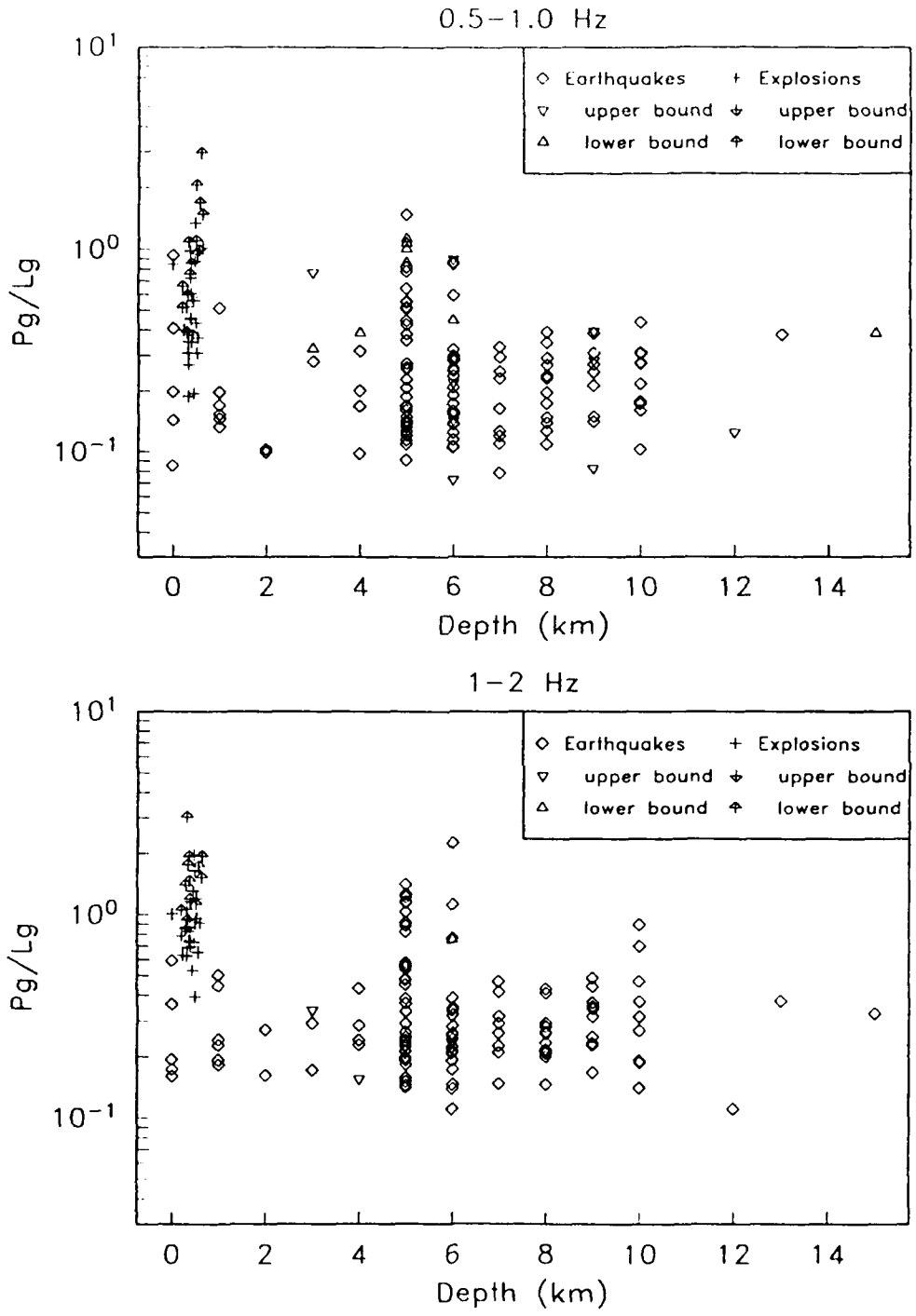

Figure 9. *Pg/Lg* ratios for all events plotted vs. source depth for the 0.5-1.0 Hz and 1-2 Hz bands. Symbols are the same as in Figure 3.

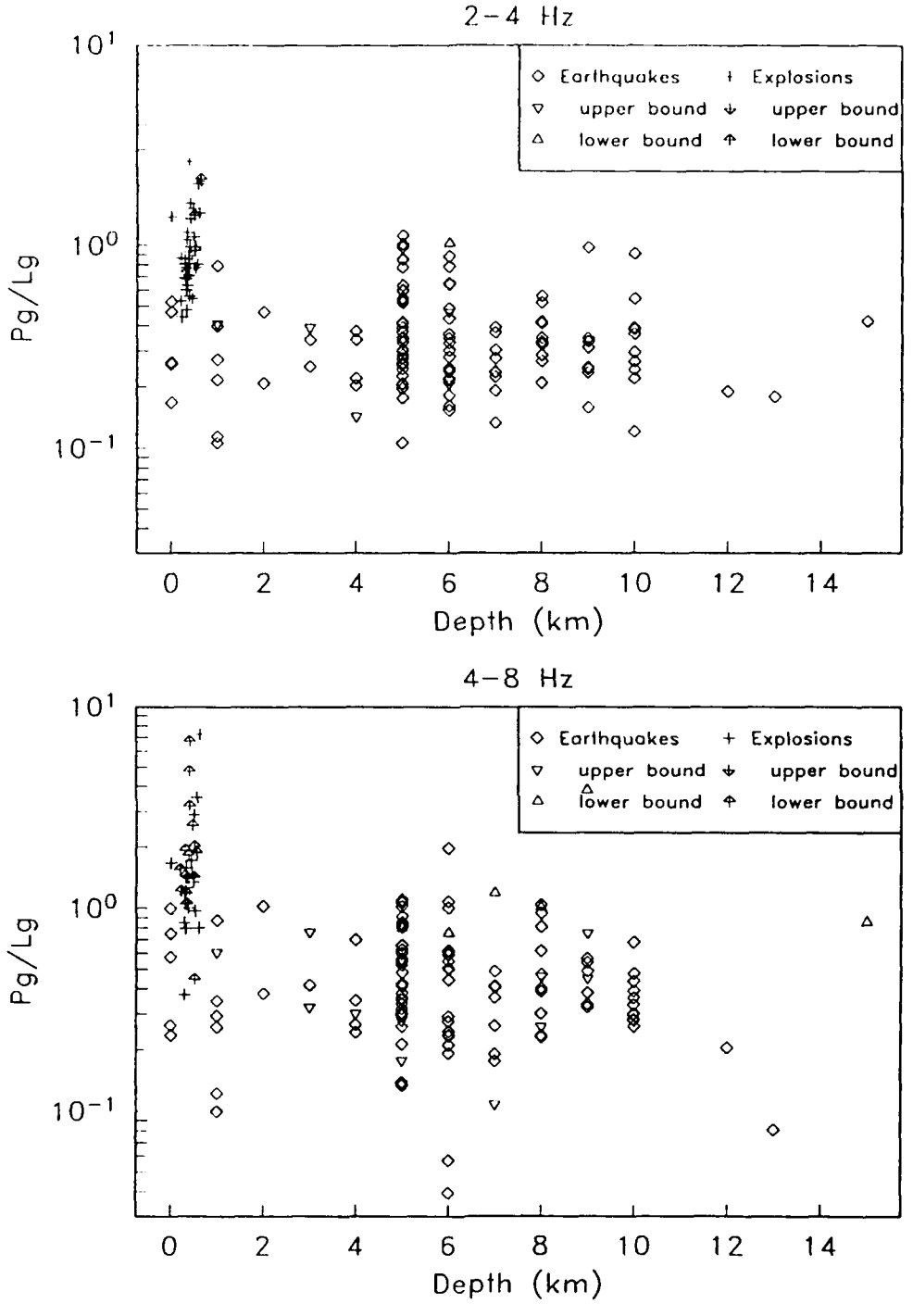

Figure 10. Same as Figure 9 for the 2-4 Hz and 4-8 Hz bands.

Variations in *Pg/Lg* with Path

One of the inherent difficulties in a discrimination study is accounting for path effects. Since the earthquakes and explosions are very often located in different regions, it is even conceivable that observed differences in phase ratios between the two populations may be due largely to differences in path rather than differences in source type. The logarithms of the uncensored phase ratio values for four frequency bands are shown on a map of the California-Nevada region in Figures 11 and 12. The mean log ratio has been removed to emphasize variations. Due to the close spacing at NTS, the mean log ratio for the explosions is shown rather than the individual values.

Two main groups can be defined according to the source-station travel path: a northerly group (above 36.5° N), which includes the explosions at the Nevada Test Site; and a more southerly group consisting of earthquakes along the Sierra-Nevada fault and in the Mojave Desert. In the lowest frequency band, events in the southerly group have mostly lower than average *Pg/Lg* ratios. In the 1-2 Hz band, a trend of increasing *Pg/Lg* with distance is visible for the southerly group, which grows stronger with increasing frequency. Thus, *Pg* propagates more efficiently than *Lg* for this group of events. This discrepancy may be due either to differences in geometric spreading (elastic effects) or attenuation (anelastic effects). The increase of the discrepancy with increasing frequency suggests that attenuation is the main cause. On the other hand, sources in the the northerly group, including the explosions at NTS, have almost uniformly higher than average *Pg/Lg* ratios at all frequencies, with little apparent distance trend.

The most striking feature of these maps is the differences between the two groups. The implication is that the path exerts a dominant effect on the *Pg/Lg* ratio. Despite the fact that

the two groups of sources are not very far apart, the paths from source to receiver are quite different due to the Sierra-Nevada batholith. It would seem that the *Lg* wavetrain for the southern group should travel along either the Sierra Nevada batholith or, more likely, along the Great Valley for most of its path. The *Lg* wavetrain from sources in the northern group, however, first traverses basin and range terrain, and then the Sierra Nevada batholith. In essence, *Lg* from the first group travels with the tectonic and topographic grain, while *Lg* from the northern sources travels across the grain. Since *Lg* is essentially a guided wave, the latter path type is likely to disrupt *Lg*, which was demonstrated by Kennett *et al.* (1990) using 3-D raytracing. In addition, *Lg* from many of the northern sources travels through the vicinity of the Mono Lakes region, where high attenuation may further decrease the *Lg* amplitude relative to *Pg*.

In contrast to the differences between the northern and southern groups of events, the average explosion *Pg/Lg* is actually quite similar to that of the earthquakes in the same region in most of the frequency bands. Only in the highest frequency band does the average *Pg/Lg* ratio appear to be higher than most of the earthquake *Pg/Lg* ratios in the same region.

We have computed maximum-likelihood averages for the explosions and both the northern and southern groups of earthquakes (Figure 13, Table 3), using the technique outlined by Jih and Shumway (1989). The error bars indicate the standard deviations of the maximum-likelihood estimates. Up to 4 Hz, the explosion population overlaps significantly with the northern group of earthquakes, while it appears to be distinct from the southern group. Note also that the differences between the northern and southern groups of earthquakes are comparable to those between the explosions and northern earthquakes. This suggests that the travel path is as important as the source type in determining the *Pg/Lg* ratio. In the highest fre-

quency band, however, the two earthquake groups converge, and the explosion Pg/Lg ratio diverges from that of the earthquakes.

Table 3. Maximum-likelihood estimates of log(Pg/Lg) averages.

	Explosions			Earthquakes (north)			Earthquakes (south)		
frequency band (Hz)	average	standard deviation	n	average	standard deviation	n	average	standard deviation	n
0.5-1.0	-0.125	0.347	43	-0.341	0.308	35	-0.726	0.226	101
1-2	0.041	0.229	43	-0.223	0.262	35	-0.614	0.178	101
2-4	-0.026	0.191	43	-0.303	0.246	35	-0.569	0.173	101
4-8	0.460	0.461	39	-0.281	0.347	34	-0.427	0.308	96

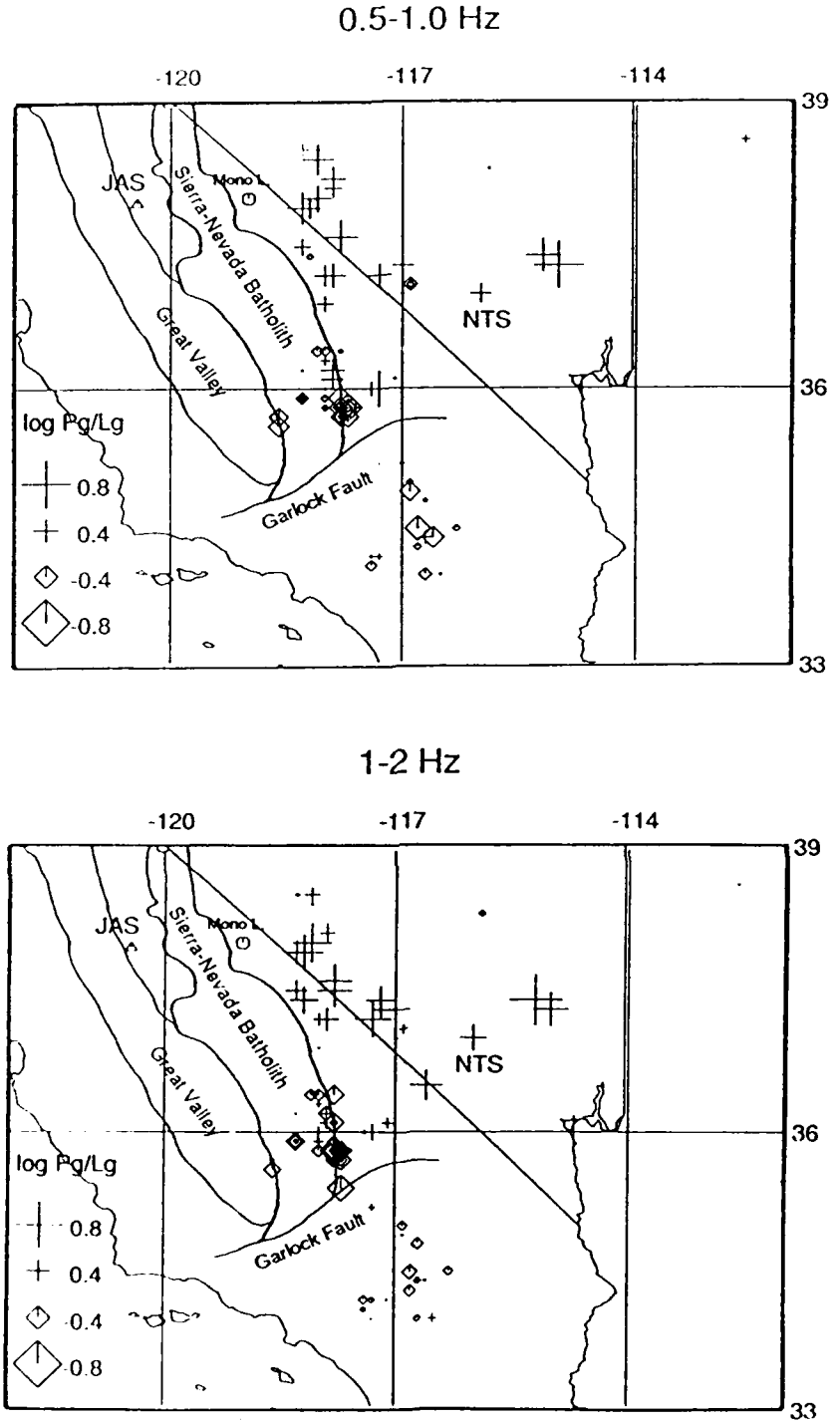

Figure 11. Variations in log(*Pg/Lg*) with location for the 0.5-1.0 Hz and 1-2 Hz bands. The mean has been removed, so that diamonds indicate lower than average *Pg/Lg* ratios and crosses indicate higher than average *Pg/Lg* ratios. For clarity, the mean of the explosions is shown, labeled NTS, instead of the individual values.

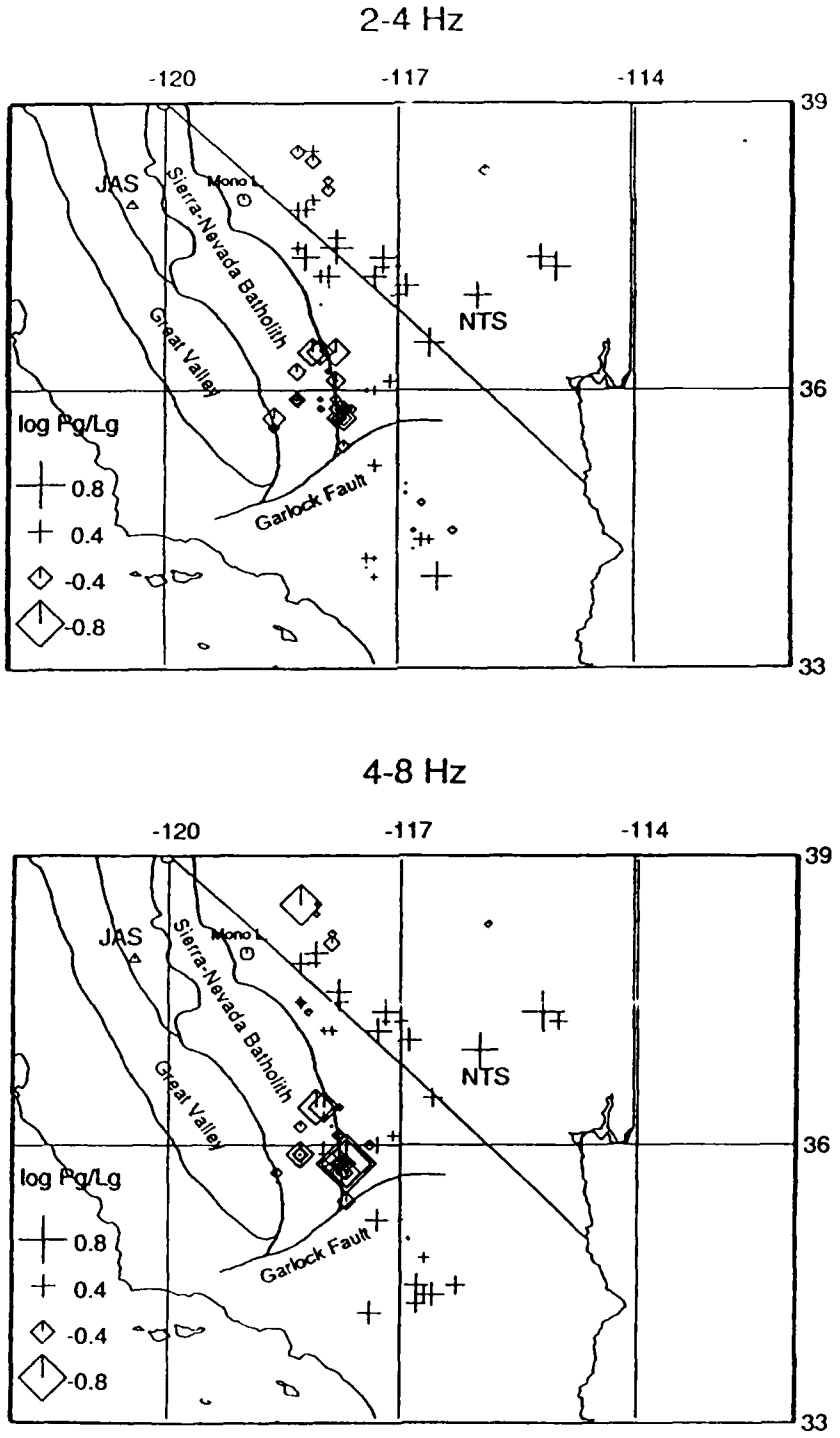

Figure 12. Same as Figure 11 for the 2-4 Hz and 4-8 Hz bands.

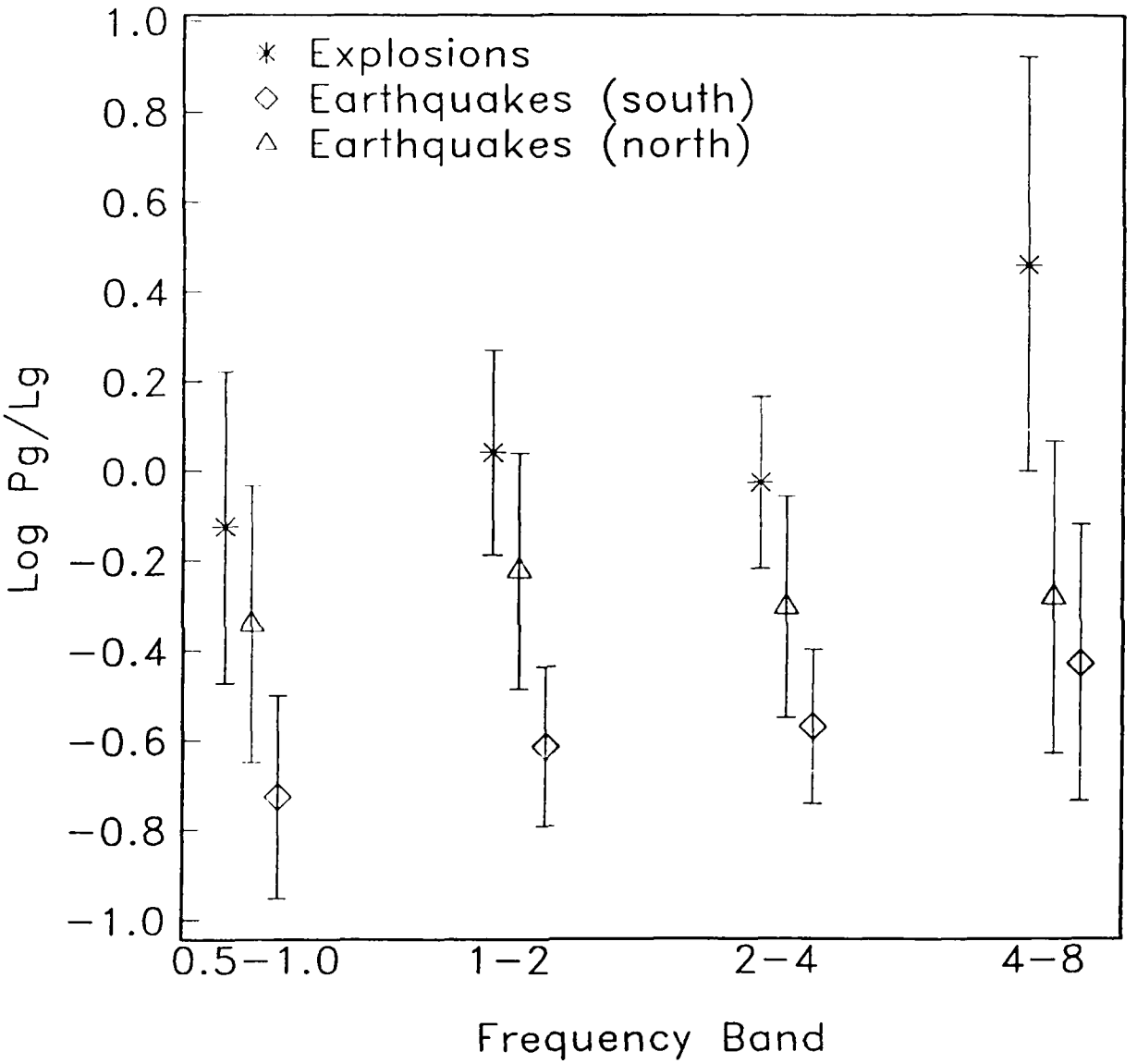

Figure 13. Maximum-likelihood estimation (MLE) of average values of log(*Pg/Lg*) for three populations: explosions (asterisks), earthquakes from the southern (California) group (diamonds), and earthquakes from the northern (Nevada) group (triangles). The error bars indicate the MLE standard deviations.

Comparison of Explosions and Collapses

One case does exist that can be used to remove the path effect entirely: a comparison of explosions with their resultant collapses. Indeed, the only difference between the explosion and the collapse should be the source function. An explosion is roughly isotropic, with a very short time history. The source mechanism of a collapse, however, is less well known, and may range anywhere from a downward point force at the cavity to a spall-like failure of near-surface rock layers. Thus the effective depth of the collapse will be less than or equal to the depth of the explosion. The symmetry of the collapse source is most probably cylindrical rather than spherical and may thus be expected to generate significant SV waves.

Three of the explosions in this data set had collapses which were well-recorded at JAS. A comparison of the *Pg* spectra for the TAJO explosion and resultant collapse is shown in Figure 14. The spectra have been smoothed with a three-point running average. The collapse is significantly depleted in high frequencies relative to the explosion, to the point where the signal-to-noise ratio is less than 1 above 4 Hz. Figure 15 shows the *Pg/Lg* ratios for the three explosion/collapse pairs, which have been smoothed with a five-point running average and offset by a factor of 10 for each pair.

The collapse ratios track those of the explosions fairly closely up to 4 Hz, despite presumably disparate source functions, emphasizing the dominant roles of path and perhaps source depth in determining *Pg/Lg* ratios. Interestingly, all of the collapse *Pg/Lg* ratios are lower than the corresponding explosion ratios at the low-frequency end. Recalling that explosion *Pg/Lg* generally increases with depth (Figures 7 and 8), this may reflect a shallower effective depth for the low-frequency component of the collapse, with the high-frequency component having a depth similar to that of the explosion.

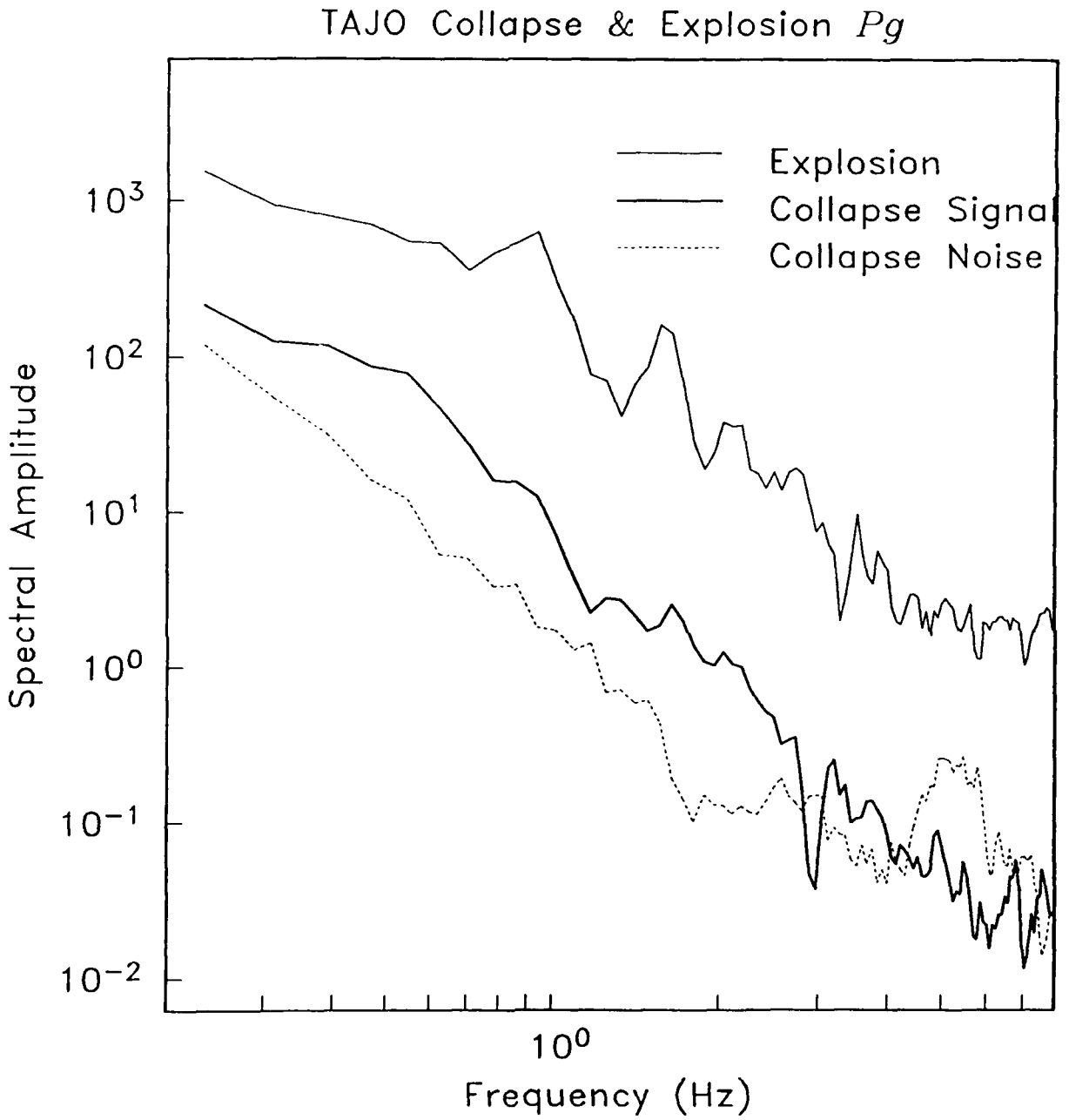

Figure 14. Comparison of TAJO collapse (heavy line) and explosion (thin line) *Pg* spectra. The dashed line is the noise spectrum of the collapse seismogram. All of the spectra have been smoothed with a three-point running average.

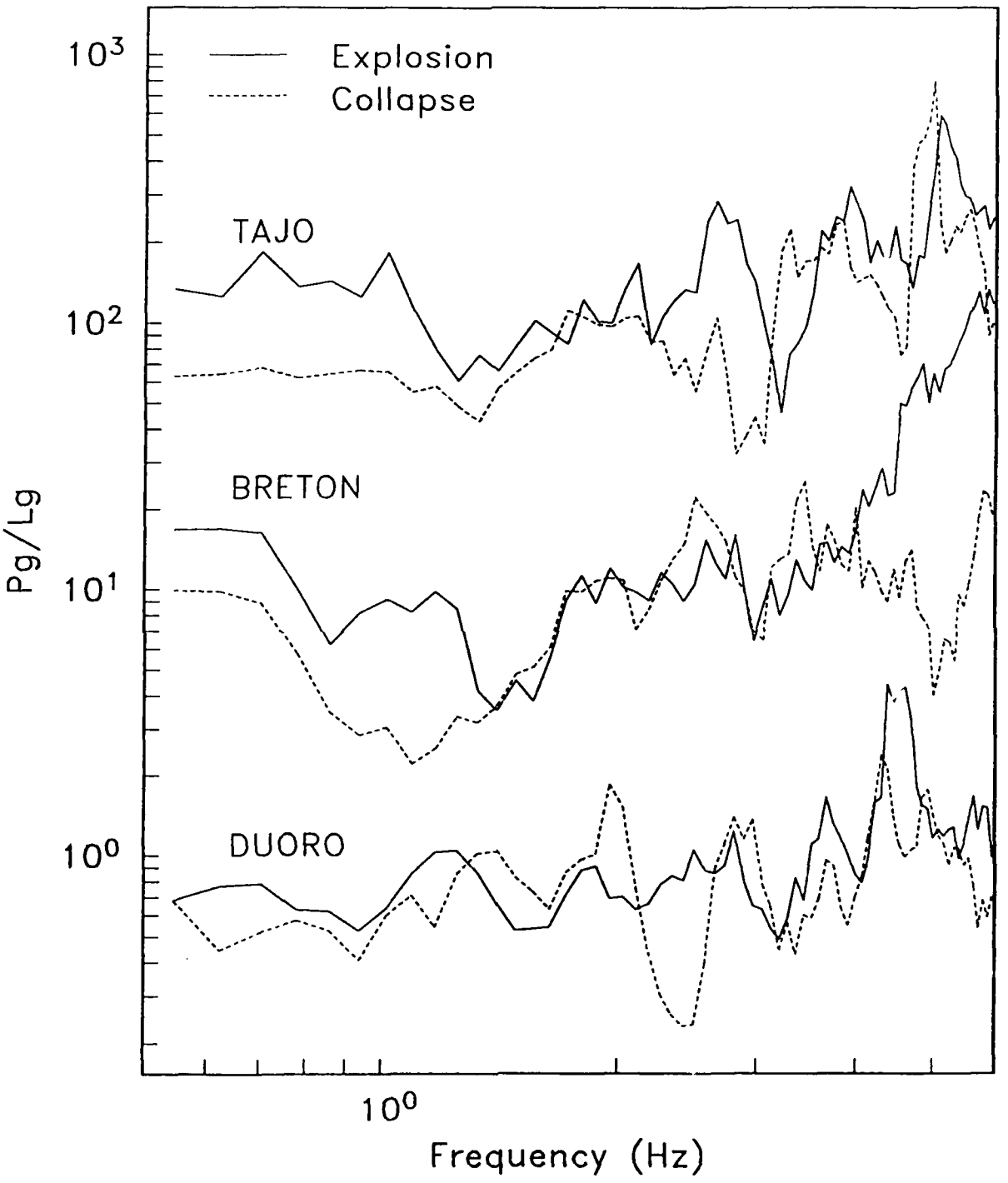

Figure 15. Comparison of explosion (solid line) and collapse (dashed line) *Pg/Lg* ratios as a function of frequency. BRETON and TAJO have been offset by respective factors of 10 and 100 from DUORO. All ratios have been smoothed with a five-point running average.

CONCLUSION

The results above shed some light on why the performance of the *Pg/Lg* discriminant is so uneven. In this case, sources were selected to be as close to each other as possible, thus reducing factors induced by azimuthally varying receiver functions and ideally mitigating the effects of the travel path. Nevertheless, sources located as little as 100 km apart have significantly different *Pg/Lg* ratios. If the set of sources is restricted only to sources that travel roughly the same path (the northern group of earthquakes), then the differences between earthquakes and explosions decrease dramatically.

These results also present grounds for both skepticism and hope in *Pg/Lg* discriminants. On one hand, the *Pg/Lg* ratios for earthquakes and explosions seem to be controlled more strongly by the travel path than the source type at most frequencies. Complicating matters further is the dependence of the explosion *Pg/Lg* ratio on source depth and/or magnitude, which tends to make shallower, smaller explosions look more like earthquakes. On the other hand, the highest frequency range studied, 4-8 Hz, seems to show some promise in that the *Pg/Lg* ratio depends somewhat less on path than in other frequency bands. Also, the explosion population is better separated from the earthquakes in this band. Still higher frequencies may improve this separation, but they could not be used for JAS, for which the sample rate was only 20 samples/second. However, the *Pg/Lg* ratio at higher frequencies also shows a stronger dependency on distance, probably due to the differential attenuation of the two phases. Thus, distance corrections may further increase the separation of earthquakes and explosions, with the caveat that these distance corrections will likely be path-dependent. Another drawback to the higher frequencies is an apparent increase in scatter for both earthquakes and explosions, and in some cases a lower signal-to-noise ratio.

ACKNOWLEDGEMENTS

The authors thank I. N. Gupta for valuable discussions, and R.-S. Jih for assistance in the application of the maximum-likelihood estimation. This research was funded by the Defense Advanced Research Projects Agency and monitored by the Air Force Geophysics Laboratory under Contract F19628-89-C-0063 (Task 2). The views and conclusions contained in this report are those of the authors and should not be interpreted as representing the official policies, either expressed or implied, of the Defense Advanced Research Projects Agency of the U. S. Government.

REFERENCES

Bennett, T. J. and J. R. Murphy (1986). Analysis of seismic discrimination capabilities using regional data from western United States events, *Bull. Seism. Soc. Am.*, **76**, 1069-1086.

Bracewell, R. N. (1986). *The Hartley Transform*, New York: Oxford University Press, 160 p.

Dysart, P. and J. Pulli (1987). Spectral study of regional earthquakes and chemical explosions recorded at the NORESS array, in: *Technical Report C87-03*, Center for Seismic Studies, Arlington, Virginia.

Dysart, P. and J. Pulli (1988). Spectral study of regional earthquakes and chemical explosions recorded at the NORESS array, in: *Technical Report C88-01*, Center for Seismic Studies, Arlington, Virginia.

Frankel, A. (1989). Effects of source depth and crustal structure on the spectra of regional phases determined from synthetic seismograms, *DARPA/AFTAC Annual Research Review for FY89*, 97-118.

Hutchenson, K. and G. Kraft, (1986). Maximum likelihood magnitudes and discrimination of regional phases, *Final Report DCS-SFR-86-01*, ENSCO, Springfield, Virginia.

Jih, R.-S. and R. H. Shumway (1989). Iterative network magnitude estimation and uncertainty assessment with noisy and clipped data, *Bull. Seism. Soc. Am.*, **79**, 1122-1141.

Lilwall, R. C. (1988). Regional *mb:Ms, Lg/Pg* amplitude ratios and *Lg* spectral ratios as criteria for distinguishing between earthquakes and explosions: a theoretical study, *Geophys. J. Roy. Astr. Soc.*, **93**, 137-147.

Kennett, B. L. N., M. G. Bostock and J.-K. Xie (1990). Guided-wave tracking in 3-D: a tool for interpreting complex regional seismograms, *Bull. Seism. Soc. Am.*, **80**, 633-642.

Pomeroy, P. W., W. J. Best and T. V. McEvilly (1982). Test ban treaty verification with regional data — a review, *Bull. Seism. Soc. Am.*, **72**, *S89-S129*.

Taylor, S. R., M. D. Denny, E. S. Vergino and R. E. Glaser (1989). Regional discrimination between NTS explosions and western U. S. earthquakes, *Bull. Seism. Soc. Am.*, **79**, 1142-1176.

(THIS PAGE INTENTIONALLY LEFT BLANK)

CONTRACTORS (United States)

Prof. Thomas Ahrens
Seismological Lab, 252-21
Division of Geological & Planetary Sciences
California Institute of Technology
Pasadena, CA 91125

Prof. Charles B. Archambeau
CIRES
University of Colorado
Boulder, CO 80309

Dr. Thomas C. Bache, Jr.
Science Applications Int'l Corp.
10260 Campus Point Drive
San Diego, CA 92121 (2 copies)

Prof. Muawia Barazangi
Institute for the Study of the Continent
Cornell University
Ithaca, NY 14853

Dr. Douglas R. Baumgardt
ENSCO, Inc
5400 Port Royal Road
Springfield, VA 22151-2388

Prof. Jonathan Berger
IGPP, A-025
Scripps Institution of Oceanography
University of California, San Diego
La Jolla, CA 92093

Dr. Lawrence J. Burdick
Woodward-Clyde Consultants
566 El Dorado Street
Pasadena, CA 91109-3245

Dr. Karl Coyner
New England Research, Inc.
76 Olcott Drive
White River Junction, VT 05001

Prof. Vernon F. Cormier
Department of Geology & Geophysics
U-45, Room 207
The University of Connecticut
Storrs, CT 06268

Professor Anton W. Dainty
Earth Resources Laboratory
Massachusetts Institute of Technology
42 Carleton Street
Cambridge, MA 02142

Prof. Steven Day
Department of Geological Sciences
San Diego State University
San Diego, CA 92182

Dr. Zoltan A. Der
ENSCO, Inc.
5400 Port Royal Road
Springfield, VA 22151-2388

Prof. John Ferguson
Center for Lithospheric Studies
The University of Texas at Dallas
P.O. Box 830688
Richardson, TX 75083-0688

Prof. Stanley Flatte
Applied Sciences Building
University of California
Santa Cruz, CA 95064

Dr. Alexander Florence
SRI International
333 Ravenswood Avenue
Menlo Park, CA 94025-3493

Prof. Stephen Grand
University of Texas at Austin
Department of Geological Sciences
Austin, TX 78713-7909

Prof. Henry L. Gray
Vice Provost and Dean
Department of Statistical Sciences
Southern Methodist University
Dallas, TX 75275

Dr. Indra Gupta
Teledyne Geotech
314 Montgomery Street
Alexandria, VA 22314

Prof. David G. Harkrider
Seismological Laboratory
Division of Geological & Planetary Sciences
California Institute of Technology
Pasadena, CA 91125

Prof. Donald V. Helmberger
Seismological Laboratory
Division of Geological & Planetary Sciences
California Institute of Technology
Pasadena, CA 91125

Prof. Eugene Herrin
Institute for the Study of Earth and Man
GeophysicalLaboratory
Southern Methodist University
Dallas, TX 75275

Prof. Robert B. Herrmann
Department of Earth & Atmospheric Sciences
St. Louis University
St. Louis, MO 63156

Prof. Bryan Isacks
Cornell University
Department of Geological Sciences
SNEE Hall
Ithaca, NY 14850

Dr. Rong-Song Jih
Teledyne Geotech
314 Montgomery Street
Alexandria, VA 22314

Prof. Lane R. Johnson
Seismographic Station
University of California
Berkeley, CA 94720

Prof. Alan Kafka
Department of Geology & Geophysics
Boston College
Chestnut Hill, MA 02167

Dr. Richard LaCoss
MIT-Lincoln Laboratory
M-200B
P. O. Box 73
Lexington, MA 02173-0073 (3 copies)

Prof Fred K. Lamb
University of Illinois at Urbana-Champaign
Department of Physics
1110 West Green Street
Urbana, IL 61801

Prof. Charles A. Langston
Geosciences Department
403 Deike Building
The Pennsylvania State University
University Park, PA 16802

Prof. Thorne Lay
Institute of Tectonics
Earth Science Board
University of California, Santa Cruz
Santa Cruz, CA 95064

Prof. Arthur Lerner-Lam
Lamont-Doherty Geological Observatory
of Columbia University
Palisades, NY 10964

Dr. Christopher Lynnes
Teledyne Geotech
314 Montgomery Street
Alexandria, VA 22314

Prof. Peter Malin
University of California at Santa Barbara
Institute for Crustal Studies
Santa Barbara, CA 93106

Dr. Randolph Martin, III
New England Research, Inc.
76 Olcott Drive
White River Junction, VT 05001

Dr. Gary McCartor
Mission Research Corporation
735 State Street
P.O. Drawer 719
Santa Barbara, CA 93102 (2 copies)

Prof. Thomas V. McEvilly
Seismographic Station
University of California
Berkeley, CA 94720

Dr. Keith L. McLaughlin
S-CUBED
A Division of Maxwell Laboratory
P.O. Box 1620
La Jolla, CA 92038-1620

Prof. William Menke
Lamont-Doherty Geological Observatory
of Columbia University
Palisades, NY 10964

Stephen Miller
SRI International
333 Ravenswood Avenue
Box AF 116
Menlo Park, CA 94025-3493

Prof. Bernard Minster
IGPP, A-025
Scripps Institute of Oceanography
University of California, San Diego
La Jolla, CA 92093

Prof. Brian J. Mitchell
Department of Earth & Atmospheric Sciences
St. Louis University
St. Louis, MO 63156

Mr. Jack Murphy
S-CUBED, A Division of Maxwell Laboratory
11800 Sunrise Valley Drive
Suite 1212
Reston, VA 22091 (2 copies)

Dr. Bao Nguyen
GL/LWH
Hanscom AFB, MA 01731-5000

Prof. John A. Orcutt
IGPP, A-025
Scripps Institute of Oceanography
University of California, San Diego
La Jolla, CA 92093

Prof. Keith Priestley
University of Cambridge
Bullard Labs, Dept. of Earth Sciences
Madingley Rise, Madingley Rd.
Cambridge CB3 OEZ, ENGLAND

Prof. Paul G. Richards
L-210
Lawrence Livermore National Laboratory
Livermore, CA 94550

Dr. Wilmer Rivers
Teledyne Geotech
314 Montgomery Street
Alexandria, VA 22314

Prof. Charles G. Sammis
Center for Earth Sciences
University of Southern California
University Park
Los Angeles, CA 90089-0741

Prof. Christopher H. Scholz
Lamont-Doherty Geological Observatory
of Columbia University
Palisades, NY 10964

Thomas J. Sereno, Jr.
Science Application Int'l Corp.
10260 Campus Point Drive
San Diego, CA 92121

Prof. David G. Simpson
Lamont-Doherty Geological Observatory
of Columbia University
Palisades, NY 10964

Dr. Jeffrey Stevens
S-CUBED
A Division of Maxwell Laboratory
P.O. Box 1620
La Jolla, CA 92038-1620

Prof. Brian Stump
Institute for the Study of Earth & Man
Geophysical Laboratory
Southern Methodist University
Dallas, TX 75275

Prof. Jeremiah Sullivan
University of Illinois at Urbana-Champaign
Department of Physics
1110 West Green Street
Urbana, IL 61801

Prof. Clifford Thurber
University of Wisconsin-Madison
Department of Geology & Geophysics
1215 West Dayton Street
Madison, WS 53706

Prof. M. Nafi Toksoz
Earth Resources Lab
Massachusetts Institute of Technology
42 Carleton Street
Cambridge, MA 02142

Prof. John E. Vidale
University of California at Santa Cruz
Seismological Laboratory
Santa Cruz, CA 95064

Prof. Terry C. Wallace
Department of Geosciences
Building #77
University of Arizona
Tucson, AZ 85721

Dr. Raymond Willeman
GL/LWH
Hanscom AFB, MA 01731-5000

Dr. Lorraine Wolf
GL/LWH
Hanscom AFB, MA 01731-5000

Dr. Monem Abdel-Gawad
Rockwell International Science Center
1049 Camino Dos Rios
Thousand Oaks, CA 91360

Prof. Keiiti Aki
Center for Earth Sciences
University of Southern California
University Park
Los Angeles, CA 90089-0741

Prof. Shelton S. Alexander
Geosciences Department
403 Deike Building
The Pennsylvania State University
University Park, PA 16802

Dr. Kenneth Anderson
BBNSTC
Mail Stop 14/1B
Cambridge, MA 02238

Dr. Ralph Archuleta
Department of Geological Sciences
University of California at Santa Barbara
Santa Barbara, CA 93102

J. Barker
Department of Geological Sciences
State University of New York
at Binghamton
Vestal, NY 13901

Dr. T.J. Bennett
S-CUBED
A Division of Maxwell Laboratory
11800 Sunrise Valley Drive, Suite 1212
Reston, VA 22091

Mr. William J. Best
907 Westwood Drive
Vienna, VA 22180

Dr. N. Biswas
Geophysical Institute
University of Alaska
Fairbanks, AK 99701

Dr. G.A. Bollinger
Department of Geological Sciences
Virginia Polytechnical Institute
21044 Derring Hall
Blacksburg, VA 24061

Dr. Stephen Bratt
Center for Seismic Studies
1300 North 17th Street
Suite 1450
Arlington, VA 22209

Michael Browne
Teledyne Geotech
3401 Shiloh Road
Garland, TX 75041

Mr. Roy Burger
1221 Serry Road
Schenectady, NY 12309

Dr. Robert Burridge
Schlumberger-Doll Research Center
Old Quarry Road
Ridgefield, CT 06877

Dr. Jerry Carter
Rondout Associates
P.O. Box 224
Stone Ridge, NY 12484

Dr. W. Winston Chan
Teledyne Geotech
314 Montgomery Street
Alexandria, VA 22314-1581

Dr. Theodore Cherry
Science Horizons, Inc.
710 Encinitas Blvd., Suite 200
Encinitas, CA 92024 (2 copies)

Prof. Jon F. Claerbout
Department of Geophysics
Stanford University
Stanford, CA 94305

Prof. Robert W. Clayton
Seismological Laboratory
Division of Geological & Planetary Sciences
California Institute of Technology
Pasadena, CA 91125

Prof. F. A. Dahlen
Geological and Geophysical Sciences
Princeton University
Princeton, NJ 08544-0636

Prof. Adam Dziewonski
Hoffman Laboratory
Harvard University
20 Oxford St
Cambridge, MA 02138

Prof. John Ebel
Department of Geology & Geophysics
Boston College
Chestnut Hill, MA 02167

Eric Fielding
SNEE Hall
INSTOC
Cornell University
Ithaca, NY 14853

Prof. Donald Forsyth
Department of Geological Sciences
Brown University
Providence, RI 02912

Dr. Cliff Frolich
Institute of Geophysics
8701 North Mopac
Austin, TX 78759

Dr. Anthony Gangi
Texas A&M University
Department of Geophysics
College Station, TX 77843

Dr. Freeman Gilbert
Inst. of Geophysics & Planetary Physics
University of California, San Diego
P.O. Box 109
La Jolla, CA 92037

Mr. Edward Giller
Pacific Sierra Research Corp.
1401 Wilson Boulevard
Arlington, VA 22209

Dr. Jeffrey W. Given
SAIC
10260 Campus Point Drive
San Diego, CA 92121

Prof. Roy Greenfield
Geosciences Department
403 Deike Building
The Pennsylvania State University
University Park, PA 16802

Dan N. Hagedorn
Battelle
Pacific Northwest Laboratories
Battelle Boulevard
Richland, WA 99352

Kevin Hutchenson
Department of Earth Sciences
St. Louis University
3507 Laclede
St. Louis, MO 63103

Prof. Thomas H. Jordan
Department of Earth, Atmospheric
and Planetary Sciences
Massachusetts Institute of Technology
Cambridge, MA 02139

Robert C. Kemerait
ENSCO, Inc.
445 Pineda Court
Melbourne, FL 32940

William Kikendall
Teledyne Geotech
3401 Shiloh Road
Garland, TX 75041

Prof. Leon Knopoff
University of California
Institute of Geophysics & Planetary Physics
Los Angeles, CA 90024

Prof. L. Timothy Long
School of Geophysical Sciences
Georgia Institute of Technology
Atlanta, GA 30332

Prof. Art McGarr
Mail Stop 977
Geological Survey
345 Middlefield Rd.
Menlo Park, CA 94025

Dr. George Mellman
Sierra Geophysics
11255 Kirkland Way
Kirkland, WA 98033

Prof. John Nabelek
College of Oceanography
Oregon State University
Corvallis, OR 97331

Prof. Geza Nagy
University of California, San Diego
Department of Ames, M.S. B-010
La Jolla, CA 92093

Prof. Amos Nur
Department of Geophysics
Stanford University
Stanford, CA 94305

Prof. Jack Oliver
Department of Geology
Cornell University
Ithaca, NY 14850

Prof. Robert Phinney
Geological & Geophysical Sciences
Princeton University
Princeton, NJ 08544-0636

Dr. Paul Pomeroy
Rondout Associates
P.O. Box 224
Stone Ridge, NY 12484

Dr. Jay Pulli
RADIX System, Inc.
2 Taft Court, Suite 203
Rockville, MD 20850

Dr. Norton Rimer
S-CUBED
A Division of Maxwell Laboratory
P.O. Box 1620
La Jolla, CA 92038-1620

Prof. Larry J. Ruff
Department of Geological Sciences
1006 C.C. Little Building
University of Michigan
Ann Arbor, MI 48109-1063

Dr. Richard Sailor
TASC Inc.
55 Walkers Brook Drive
Reading, MA 01867

John Sherwin
Teledyne Geotech
3401 Shiloh Road
Garland, TX 75041

Prof. Robert Smith
Department of Geophysics
University of Utah
1400 East 2nd South
Salt Lake City, UT 84112

Prof. S. W. Smith
Geophysics Program
University of Washington
Seattle, WA 98195

Dr. Stewart W. Smith
Geophysics AK-50
University of Washington
Seattle, WA 98195

Dr. George Sutton
Rondout Associates
P.O. Box 224
Stone Ridge, NY 12484

Prof. L. Sykes
Lamont-Doherty Geological Observatory
of Columbia University
Palisades, NY 10964

Prof. Pradeep Talwani
Department of Geological Sciences
University of South Carolina
Columbia, SC 29208

Prof. Ta-liang Teng
Center for Earth Sciences
University of Southern California
University Park
Los Angeles, CA 90089-0741

Dr. R.B. Tittmann
Rockwell International Science Center
1049 Camino Dos Rios
P.O. Box 1085
Thousand Oaks, CA 91360

Dr. Gregory van der Vink
IRIS, Inc.
1616 North Fort Myer Drive
Suite 1440
Arlington, VA 22209

Professor Daniel Walker
University of Hawaii
Institute of Geophysics
Honolulu, HI 96822

William R. Walter
Seismological Laboratory
University of Nevada
Reno, NV 89557

Dr. Gregory Wojcik
Weidlinger Associates
4410 El Camino Real
Suite 110
Los Altos, CA 94022

Prof. John H. Woodhouse
Hoffman Laboratory
Harvard University
20 Oxford St.
Cambridge, MA 02138

Prof. Francis T. Wu
Department of Geological Sciences
State University of New York
at Binghamton
Vestal, NY 13901

Dr. Gregory B. Young
ENSCO, Inc.
5400 Port Royal Road
Springfield, VA 22151-2388

Dr. Ralph Alewine III
DARPA/NMRO
1400 Wilson Boulevard
Arlington, VA 22209-2308

Mr. James C. Battis
GL/LWH
Hanscom AFB, MA 01731-5000

Dr. Robert Blandford
DARPA/NMRO
1400 Wilson Boulevard
Arlington, VA 22209-2308

Eric Chael
Division 9241
Sandia Laboratory
Albuquerque, NM 87185

Dr. John J. Cipar
GL/LWH
Hanscom AFB, MA 01731-5000

Mr. Jeff Duncan
Office of Congressman Markey
2133 Rayburn House Bldg.
Washington, DC 20515

Dr. Jack Evernden
USGS - Earthquake Studies
345 Middlefield Road
Menlo Park, CA 94025

Art Frankel
USGS
922 National Center
Reston, VA 22092

Dr. T. Hanks
USGS
Nat'l Earthquake Research Center
345 Middlefield Road
Menlo Park, CA 94025

Dr. James Hannon
Lawrence Livermore Nat'l Laboratory
P.O. Box 808
Livermore, CA 94550

Paul Johnson
ESS-4, Mail Stop J979
Los Alamos National Laboratory
Los Alamos, NM 87545

Janet Johnston
GL/LWH
Hanscom AFB, MA 01731-5000

Dr. Katharine Kadinsky-Cade
GL/LWH
Hanscom AFB, MA 01731-5000

Ms. Ann Kerr
IGPP, A-025
Scripps Institute of Oceanography
University of California, San Diego
La Jolla, CA 92093

Dr. Max Koontz
US Dept of Energy/DP 5
Forrestal Building
1000 Independence Avenue
Washington, DC 20585

Dr. W.H.K. Lee
Office of Earthquakes, Volcanoes,
& Engineering
345 Middlefield Road
Menlo Park, CA 94025

Dr. William Leith
U.S. Geological Survey
Mail Stop 928
Reston, VA 22092

Dr. Richard Lewis
Director, Earthquake Engineering & Geophysics
U.S. Army Corps of Engineers
Box 631
Vicksburg, MS 39180

James F. Lewkowicz
GL/LWH
Hanscom AFB, MA 01731-5000

Mr. Alfred Lieberman
ACDA/VI-OA'State Department Bldg
Room 5726
320 - 21st Street, NW
Washington, DC 20451

Stephen Mangino
GL/LWH
Hanscom AFB, MA 01731-5000

Dr. Robert Masse
Box 25046, Mail Stop 967
Denver Federal Center
Denver, CO 80225

Art McGarr
U.S. Geological Survey, MS-977
345 Middlefield Road
Menlo Park, CA 94025

Richard Morrow
ACDA/VI, Room 5741
320 21st Street N.W
Washington, DC 20451

Dr. Keith K. Nakanishi
Lawrence Livermore National Laboratory
P.O. Box 808, L-205
Livermore, CA 94550

Dr. Carl Newton
Los Alamos National Laboratory
P.O. Box 1663
Mail Stop C335, Group ESS-3
Los Alamos, NM 87545

Dr. Kenneth H. Olsen
Los Alamos Scientific Laboratory
P.O. Box 1663
Mail Stop C335, Group ESS-3
Los Alamos, NM 87545

Howard J. Patton
Lawrence Livermore National Laboratory
P.O. Box 808, L-205
Livermore, CA 94550

Mr. Chris Paine
Office of Senator Kennedy
SR 315
United States Senate
Washington, DC 20510

Colonel Jerry J. Perrizo
AFOSR/NP, Building 410
Bolling AFB
Washington, DC 20332-6448

Dr. Frank F. Pilotte
HQ AFTAC/TT
Patrick AFB, FL 32925-6001

Katie Poley
CIA-OSWR/NED
Washington, DC 20505

Mr. Jack Rachlin
U.S. Geological Survey
Geology, Rm 3 C136
Mail Stop 928 National Center
Reston, VA 22092

Dr. Robert Reinke
WL/NTESG
Kirtland AFB, NM 87117-6008

Dr. Byron Ristvet
HQ DNA, Nevada Operations Office
Attn: NVCG
P.O. Box 98539
Las Vegas, NV 89193

Dr. George Rothe
HQ AFTAC/TGR
Patrick AFB, FL 32925-6001

Dr. Alan S. Ryall, Jr.
DARPA/NMRO
1400 Wilson Boulevard
Arlington, VA 22209-2308

Dr. Michael Shore
Defense Nuclear Agency/SPSS
6801 Telegraph Road
Alexandria, VA 22310

Donald L. Springer
Lawrence Livermore National Laboratory
P.O. Box 808, L-205
Livermore , CA 94550

Mr. Charles L. Taylor
GL/LWG
Hanscom AFB, MA 01731-5000

Dr. Thomas Weaver
Los Alamos National Laboratory
P.O. Box 1663, Mail Stop C335
Los Alamos, NM 87545

J.J. Zucca
Lawrence Livermore National Laboratory
Box 808
Livermore, CA 94550

GL/SULL
Research Library
Hanscom AFB , MA 01731-5000 (2 copies)

Secretary of the Air Force
(SAFRD)

Washington, DC 20330

Office of the Secretary Defense
DDR & E
Washington, DC 20330

HQ DNA
Attn: Technical Library
Washington, DC 20305

DARPA/RMO/RETRIEVAL
1400 Wilson Boulevard
Arlington, VA 22209

DARPA/RMO/Security Office
1400 Wilson Boulevard
Arlington, VA 22209

Geophysics Laboratory
Attn: XO
Hanscom AFB, MA 01731-5000

Geophysics Laboratory
Attn: LW
Hanscom AFB, MA 01731-5000

DARPA/PM
1400 Wilson Boulevard
Arlington, VA 22209

Defense Technical Information Center
Cameron Station
Alexandria, VA 22314 (2 copies)

Defense Intelligence Agency
Directorate for Scientific &
Technical Intelligence/DT1B
Washington, DC 20340-6158

AFTAC/CA
(STINFO)
Patrick AFB, FL 32925-6001

TACTEC
Battelle Memorial Institute
505 King Avenue
Columbus, OH 43201 (Final Report Only)

Dr. Ramon Cabre, S.J.
Observatorio San Calixto
Casilla 5939
La Paz, Bolivia

Prof. Hans-Peter Harjes
Institute for Geophysik
Ruhr University/Bochum
P.O. Box 102148
4630 Bochum 1, FRG

Prof. Eystein Husebye
NTNF/NORSAR
P.O. Box 51
N-2007 Kjeller, NORWAY

Prof. Brian L.N. Kennett
Research School of Earth Sciences
Institute of Advanced Studies
G.P.O. Box 4
Canberra 2601, AUSTRALIA

Dr. Bernard Massinon
Societe Radiomana
27 rue Claude Bernard
75005 Paris, FRANCE (2 Copies)

Dr. Pierre Mecheler
Societe Radiomana
27 rue Claude Bernard
75005 Paris, FRANCE

Dr. Svein Mykkeltveit
NTNF/NORSAR
P.O. Box 51
N-2007 Kjeller, NORWAY

FOREIGN (Others)

Dr. Peter Basham
Earth Physics Branch
Geological Survey of Canada
1 Observatory Crescent
Ottawa, Ontario, CANADA K1A 0Y3

Dr. Eduard Berg
Institute of Geophysics
University of Hawaii
Honolulu, HI 96822

Dr. Michel Bouchon
I.R.I.G.M.-B.P. 68
38402 St. Martin D'Heres
Cedex, FRANCE

Dr. Hilmar Bungum
NTNF/NORSAR
P.O. Box 51
N-2007 Kjeller, NORWAY

Dr. Michel Campillo
Observatoire de Grenoble
I.R.I.G.M.-B.P. 53
38041 Grenoble, FRANCE

Dr. Kin Yip Chun
Geophysics Division
Physics Department
University of Toronto
Ontario, CANADA M5S 1A7

Dr. Alan Douglas
Ministry of Defense
Blacknest, Brimpton
Reading RG7-4RS, UNITED KINGDOM

Dr. Roger Hansen
NTNF/NORSAR
P.O. Box 51
N-2007 Kjeller, NORWAY

Dr. Manfred Henger
Federal Institute for Geosciences & Nat'l Res.
Postfach 510153
D-3000 Hanover 51, FRG

Ms. Eva Johannisson
Senior Research Officer
National Defense Research Inst.
P.O. Box 27322
S-102 54 Stockholm, SWEDEN

Dr. Fekadu Kebede
Seismological Section
Box 12019
S-750 Uppsala, SWEDEN

Dr. Tormod Kvaerna
NTNF/NORSAR
P.O. Box 51
N-2007 Kjeller, NORWAY

Dr. Peter Marshal
Procurement Executive
Ministry of Defense
Blacknest, Brimpton
Reading FG7-4RS, UNITED KINGDOM

Prof. Ari Ben-Menahem
Department of Applied Mathematics
Weizman Institute of Science
Rehovot, ISRAEL 951729

Dr. Robert North
Geophysics Division
Geological Survey of Canada
1 Observatory Crescent
Ottawa, Ontario, CANADA K1A 0Y3

Dr. Frode Ringdal
NTNF/NORSAR
P.O. Box 51
N-2007 Kjeller, NORWAY

Dr. Jorg Schlittenhardt
Federal Institute for Geosciences & Nat'l Res.
Postfach 510153
D-3000 Hannover 51, FEDERAL REPUBLIC OF GERMANY